THE EFFECT OF GROWTH-RESTRICTION ON THE MURINE GUT MICROBIOME

By

Melissa Quinn

A THESIS

Submitted to
Michigan State University
in partial fulfillment of the requirements
for the degree of

Kinesiology-Master of Science

2020

ABSTRACT

THE EFFECT OF GROWTH-RESTRICTION ON THE MURINE GUT MICROBIOME

By

Melissa Quinn

INTRODUCTION. Growth restriction induced by undernutrition in early life increases the risk of developing chronic diseases in adulthood. We hypothesized growth restriction would alter the gut microbiome and metabolome across the lifespan, impairing vital growth signaling processes necessary for proper development, with a primary focus on muscular and hepatic Insulin-like Growth Factor (IGF-1) expression. **METHODS.** A cross-fostering, protein-restricted nutritive model (8% protein) was used to induce undernutrition during gestation (GUN) or lactation (PUN). At 21 days of age (PN21), all mice were weaned to a control diet (CON; 20% protein), isolating undernutrition to specific windows of early life. Fecal samples were collected weekly to determine longitudinal programming effects of growth restriction on the gut microbiome (CON N=5, GUN N=6, PUN N=6) and metabolome. Liver samples were collected at PN21 (CON N=12, GUN N=6, PUN N=7) and PN80 (CON N=13, GUN N=9, PUN N=11) and analyzed along with the cecum for metabolomics via tandem mass spectrometry (LC-MS/MS) and analyzed with the Global Natural Products Social Molecular Networking (GNPS) bioinformatics software. Hepatic and gastrocnemius (GS) IGF-1 expression (CON N=15, GUN N=12, PUN N=13) was analyzed via a Total Protein NIR western blot. **RESULTS.** The fecal Beta-Diversity was separated by treatment group using Weighted UniFrac (PERMANOVA p=0.0001). Linear mixed model (LMM) analysis revealed PUN having higher abundance of specific bacteria compared to GUN and CON across the lifespan. Additionally, the PUN metabolome was significantly altered compared to GUN and CON. Western blot analysis revealed significantly lower hepatic IGF-1 expression at PN21 in GUN (p=0.0012) and PUN (p<0.001) and overall lower GS IGF-1 expression (PUN: p=0.037; GUN: p=0.007) compared to CON. **CONCLUSION:** The gut microbiome and metabolome are permanently altered by early life growth restriction.

ACKNOWLEDGMENTS

I would like to thank the current as well as former members of the Neonatal Nutrition and Exercise Research Lab for their help and support: Eric Leszczynski, Joe Visker, Austin Wellette-Hunsucker, Logan Pendergrast, Ashley McPeek and Abby Prichard. I would also like to thank Dr. Robert Quinn, Ruma Raghuvanshi and Christian Martin for providing training and assistance in the microbiome and metabolomic methods used in this study. Finally, I would like to thank the members of my thesis committee, Drs. Karin Pfeiffer, Laura McCabe and David Ferguson for their mentorship and guidance with this project.

TABLE OF CONTENTS

LIST OF TABLES

LIST OF FIGURES

KEY TO ABBREVIATIONS

IGF-1	Insulin-like Growth Factor 1
CON	Control Group
DoHAD	Developmental Origins of Health and Disease
GS	Gastrocnemius
GUN	Gestationally Undernourished Group
PN	Postnatal Day of Life in Mice
PUN	Postnatally Undernourished Group
SCFA	Short-chain Fatty Acids
EAAs	Essential Amino Acids
CA	Cholic Acid
GCA	Glycocholic Acid
MCA	Muricholic Acid
DCA	Deoxycholic Acid
TCA	Taurocholic Acid
DHEA	Dehydroepiandrosterone

INTRODUCTION

Growth restriction induced by undernutrition affects one in seven births worldwide[1]. Gestational growth restriction (GUN) results in lower birth weights and is high susceptibility to developing non-communicable metabolic diseases in adulthood (i.e. cardiovascular disease[2] and diabetes[3]). With optimal refeeding during postnatal development, catch-up growth is often achieved, although the susceptibility of chronic disease onset still remains[4,5]. Alternatively, postnatal growth restriction (PUN) results in lower body weights over the lifespan despite refeeding, indicating there is an underlying mechanism leading to a permanent reprogramming in normal growth and development processes[6,7]. In order to mitigate disease onset in the growth restricted population, mechanisms influencing growth and development must be characterized.

Growth restriction is associated with B-Vitamin deficiencies (i.e. folate or B-12)[8–11] that inhibit protein synthesis and growth[9,10]. Recent findings show that B-Vitamins are synthesized by microbes (specifically *Bifidobacterium* and *Lactobacillus*) in the digestive system[12]. These microbial strains are the greatest vitamin producers[12], suggesting their crucial role during early life growth and development.

Schwarzer et al. demonstrated that supplementation with *Lactobacillus* improved insulin-like growth factor (IGF-1) levels in liver and gastrocnemius (GS), subsequently improving physical growth in germ free mice (mice that lack a gut microbiome)[13]. Supplementation was given to the mice post-weaning (PN21) which leaves question to whether there would be stronger differences found during the developmental period (PN1-21). However, the study by Schwarzer lacked characterization of the gut microbial composition in the growth restricted mice. Therefore, we hypothesize that early life growth-restriction causes gut dysbiosis and an altered metabolome highlighted by decreased B-Vitamin bioavailability, leading to decreased IGF-1 expression and subsequent growth restriction across the lifespan.

To test this hypothesis, we have developed the following aims:

Aim 1: To determine the microbiome differences across the lifespan of mice subjected to undernutrition during gestation (GUN) or the postnatal period (PUN) compared to controls (CON). Fecal samples were collected once per week from PN18-PN80 to generate microbiome data in order to compare changes in microbial structure and diversity. Principle coordinate analysis plots (PCoA) were used to assess changes in microbial communities. We hypothesized both GUN and PUN mice would have an altered microbiome compared to controls across the lifespan characterized by a decrease in vitamin producing *Bifidobacterium* and *Lactobacilli*.

Aim 2: To determine the effects of growth restriction on metabolites produced in GUN, PUN and CON mice. Untargeted metabolomics were used to quantify molecules from cecum and liver samples at PN21 and PN80. Multivariate statistical approaches were used to determine the overall metabolomic changes as well as specific differences between those of interest (i.e. B-Vitamins). We hypothesized growth restriction will alter the metabolome. We also hypothesized the altered metabolome would be characterized by decreased levels of B-Vitamins in GUN and PUN mice.

Aim 3: To determine the effects of growth-restriction on IGF-1 abundance in liver and gastrocnemius samples using western blots at PN21 and PN80 in CON, GUN, and PUN. We hypothesized that there would be decreased levels of IGF-1 in the PUN and GUN mice, which will correlate to decreased body and muscle weight.

Completion of these aims will provide mechanistic insight regarding early life growth restriction and provide a foundation for interventions to restore microbiome dysbiosis, promote growth and reduce chronic disease development in adulthood.

LITERATURE REVIEW

The scope of this literature review is to demonstrate the significance of growth restriction in regards to public health relevance, discuss the use of animal models for growth restriction, highlight the importance of the gut microbiome in regards to growth restriction and introduce the principles of methods proposed for this thesis, thereby providing rationale for the hypothesis and aims proposed.

Epidemiological Evidence for the DoHad Hypothesis

The Developmental Origins of Health and Disease (DOHaD) hypothesis states that early life conditions, specific to the nutritive environment, can result in epigenetic programming that dictates susceptibility to disease state later in life[4,5]. Epidemiological studies, such as those from the Dutch famine, reveal early life growth restriction increases the susceptibility of developing coronary heart disease, atherogenic lipid profile, disturbed blood coagulation, hypertension, sarcopenia, obesity and even cancer[14,15]. Specifically, those exposed to the famine in late gestation exhibited impaired glucose tolerance which suggests a link to the development of diabetes later in life[15].

It is becoming apparent with increasing research on growth restriction in early life, that the actual timing of the nutritional insult is largely the determining factor in which organ system is affected[15,16]. According to the Helsinki Birth Cohort, humans that exhibited slow early fetal growth developed coronary heart disease, type 2 diabetes and had a higher incidence of stroke[17]. In addition, Sandboge et al. demonstrated that those who remained small in early childhood were highly likely to develop metabolic syndrome in adulthood and non-alcoholic fatty liver disease (NAFLD)[18]. On the other hand, those born growth restricted that exhibited rapid catch-up growth during postnatal life have been shown to accumulate more fat mass than muscle, creating a higher susceptibility to metabolic disease onset in adulthood[17]. The development of precise therapeutic methods is essential to preventing disease onset and

improve fetal and postnatal development around the globe however, the mechanisms must first be understood.

Animal Models for Growth Restriction

Animal models are vital to gaining better insight into environmental, genetic or epigenetic factors related to growth and development across the lifespan, due to the ease at which tissues can be collected. Unlike human studies, research involving animal models allows for a shorter evaluation of longitudinal data collection due to their condensed lifespans (on average 2 years). Additionally, animal models are beneficial in the ability to implement greater control over environmental variables compared to human studies[19]. Among all animal models commonly used, mice have a particular advantage over others, due to similar genetic features, anatomy, physiology, and metabolic function to humans[19]. The mice used in this study are also a genetically homozygous cohort, eliminating unwanted variables seen in human nutritional studies and allowing for testing pathophysiological mechanisms of human diseases[19].

Common methods to induce growth restriction in mice include protein or nutrient-restriction during gestation or postnatal life[3,6,7,20–26], food-restricted dams[27–31], timed separation of pups from suckling dams prior to weaning age[32–34], and intrauterine tubal ligation (IUGR)[35,36]. It is thought that with the latter two methods, there may be confounding factors correlated with hypoxic or stressful environmental effects that can increase cortisol[34,37] and glucocorticoid release[27], affecting results and increasing risk of false-positive findings. Protein and nutrient-restrictive models, especially those that are isocaloric, are low-stress alternatives to achieving the same result: growth-restricted offspring[3,20–23,26].

In terms of using mouse models for gut microbiome research, mice are omnivorous like humans and have very similar gut anatomy and physiology to humans[19,38]. Mouse models have been used for many years to study human gastrointestinal diseases and treatments due to mice showing similar pathology to genetic, nutritional or environmental changes[39–44]. The intestinal tract of a mouse is

exponentially smaller compared to other animals allowing ease of testing the entire region. Mice and humans both have overall the same GI anatomy as well as similar intestinal mucosa, lamina propria, absorptive enterocytes, goblet cells, as well as many others[19,38,39]. One distinct difference between mouse and human intestinal tracts is that mice have the cecum as a separate compartment, while humans' cecums are hardly separate from the colon; thus cecums of mice and humans serve very different functions[39]. The mouse cecum is usually known to be a place of bacterial fermentation and nutrient synthesis[39,45], while in humans the cecum still contains bacterial fermentation but not to the capacity of the human large intestines[46,47]. It is thought that over time with evolution what was once the human cecum degenerated and became an unused section that simply connects the small intestine to the large intestine[48–50]. However, further elucidating cecum functions in mice can still be translatable to human small intestine activity since it connects the small and large intestines.

Development of the Gut Microbiome

The gut microbiome, which is the consortium of thousands of microbial species residing in the mammalian gastrointestinal tract, has many functions in the host including enhancing nutrient absorption and digestion, regulating immune responses and maintaining enzymatic and cell signaling activity in the gut and liver[51]. Microbiome diversity is affected by host genetics, environment, early microbial exposure and diet[52]. The infant gut microbiome is more variable than adults[53]. The microbial community in the infant gut progressively changes through the first two years of life, due to alterations in diet and other environmental exposures[54], but after this age, the gut microbiome is highly stable throughout the lifetime[52]. In early life, there are primarily three main bacterial phyla: Actinobacteria, Firmicutes, and Bacteriodetes[52]. It has been shown that an infant's lack of overall diversity is most likely due to their diet being comprised of mainly breast milk or formula[55–57]. There is conflicting information as to the actual composition of phyla and species found, however the most commonly published microbes seen in infants are Actinobacteria and Firmicutes[32,52,58], with varying levels of *Lactobacillus and Bifidobacterium*

species[59,60]. By the pre-toddler age of 9-18 months (approximately 14 days in mice)[61], the bacteria present begin to diversify and the microbial taxa present changes. This can result in an increase in butyrate production, a vital metabolite in epithelial cell growth and renewal in the gut. A lack of butyrate-producing microbes in early life is suggested to directly affect the integrity of the gut lining and optimal nutrient absorption[62–64]. At approximately 2 years of age (or 18 days in mice)[65] the gut microbiome resembles that of an adult and establishes its stability[52]. Though much research has focused on development of the neonatal microbiome (described below), few studies have investigated how growth restriction alters this development and whether there are links between chronic diseases described above from growth restriction and gut microbiome alterations in early life.

The Influence of Growth Restriction on the Gut Microbiome

With the wide variety of external influences that shape the microbiome that occur in early life, it is likely a reduction in nutrient availability would also have lasting effects on the gut microbiome. It has been speculated that the gut microbiome, like other organs and cellular processes, may be stunted in growth restricted individuals[66]. A recent study by Schwarzer *et al.* elucidated potential mechanisms by which the gut microbiome can influence longitudinal growth. When germ-free mice were given a one-time dose of a specific strain of *Lactobacillus* prior to mating, their offspring resulted in improved growth hormone and insulin-like growth factor (IGF-1) signaling despite being fed a restricted diet from PN21 till PN56. This study by Schwarzer et al. suggests that certain gut microbes have not only the ability to induce growth by interacting with the GH-IGF1 axis but also have some protective effects against growth restriction.[13]

There are two specific phyla, Bacteroidetes and Lactobacillus, that increase B-Vitamin bioavailability in the intestinal lumen. B-12 and folate are well-known for their growth promoting properties[67]. Folate is responsible for perinatal development and regulation via DNA methylation

processes[9]. DNA methylation is crucial for normal development in mammals[9]. Although there is little information in the literature connecting dietary folate deficiency during early life, growth restriction and the gut microbiome, it is feasible that if bacteria are unable to produce these vital molecules there would be alterations in the IGF-1 growth system. Similarly, vitamin B-12 is also known for its contribution to cellular growth and energy balance regulation[68]. A study by Chen et al. 2018 showed that intrauterine growth restriction (IUGR) led to significant reductions in folate uptake as well as folate transport capacity in the placenta via reduced expression of folate receptor-α and folate carrier protein[69]. There is, unfortunately, very limited literature testing the connection between B-Vitamin transporters and postnatal growth restriction. Future studies should further examine the connections between growth restriction, gut microbes and B-Vitamin biosynthesis and transport in early life.

The impact of growth restriction on intestinal structural differences has mostly been shown in studies implementing IUGR growth restriction, which leads to significantly smaller intestinal villi[70]. Intestinal villi are not only important for nutrient absorption, but also for maintaining the mucus (mucin) layer which protects against pathogenic microbes and maintains integrity of the GI tract[71–73]. There is very limited literature available testing the effects of postnatal growth restriction on the villi or mucin layer in the intestinal tract. More information is necessary to establish a relationship between growth restriction that occurs during lactation and structural abnormalities in the intestinal tract in adulthood.

Relationship Between the Liver and the Gut Microbiome

Recent research has focused on determining the relationship between the digestive tract and the liver, better known as the gut-liver axis[74,75]. The liver and intestine are known to communicate extensively through the portal vein and biliary tract[75]. Pro-inflammatory changes in the liver and intestine due to environmental and/or genetic factors have been shown to influence the development of further disease states by increasing fibrosis, cirrhosis, and in some cases, carcinoma. There are distinct gut dysbiotic

phenotypes expressed in liver-related diseases (e.g. nonalcoholic fatty liver disease (NAFLD)), that lead to gut permeability and shifts in levels of certain key metabolites (e.g. butyrate) and leads to further disease progression, and even more serious conditions (e.g. Crohn's Disease, Leaky Gut, and Cancer)[74]. It has been shown in previous studies that addressing the health of the gut microbiome in this case can actually improve the subjects' disease state and prevent further metabolic damage[76].

In the majority of mammalian species, growth in early life is modulated through growth hormone (GH) and insulin-like growth factor (IGF-1) activity by way of paracrine and endocrine cell signaling mechanisms, or the somatotropic axis (GH-IGF)[26,77,78]. In more recent studies, nutritional status and gut microbe supplementation alters IGF-1 expression and improves bone growth, suggesting an optimal diet and gut microbiome play a large role in early life growth and development[79]. Unfortunately, most of these studies focused mostly on longitudinal growth and ossification of bones, which while highly important, still leaves inquiry as to the status of organ, muscle and tissue development[77,80].

The Role of GH, IGF-1 and Perinatal Growth

Previous studies have suggested a potential link between gestational and postnatal growth restriction and abnormal GH-IGF axis activity as a cause for low birth weight and a vital predictor of obesity, diabetes and cardiovascular disease in adulthood[81–83]. Abnormalities in the GH-IGF axis may consist of anything from decreased prevalence of certain IGF-1 receptors (IGFR) or binding proteins (IGFBP), lack of binding of IGF-1 receptors, or cellular resistance to GH in muscle and/or liver. In the case of GH tissue resistance, there is a resulting decrease in IGF-1 release, regardless of the amount of circulating GH[84]. GH is a known anabolic tissue regulator, primarily released by the pituitary gland and stimulates IGF-1 release in surrounding tissues. During gestation and postnatal life, insulin, IGF-1, and IGFBPs are main regulators of growth and development[85–87]. Additionally, in postnatal life, IGF-1

signaling may have more of an effect on protein, lipid and glucose metabolism[87], thus placing it as a major focus of the present study.

Principles of the Methods Used in this Thesis

The nutritive model used to induce growth restriction is a previously verified protocol that has been used repeatedly in various studies in the Neonatal Nutrition and Exercise Research Lab (NNERL)[6,7,88]. This model has been shown to alter the amount of nutrients received from the LP-fed mother during gestation, resulting in pups that are significantly growth restricted at PN1 (GUN)[6,7,88]. Additionally, when growth restriction is induced from PN1-21 in previously CON milk fed pups (PUN) this results in overall growth restriction of body weight[6,7,88], some organs[7], as well as reduced skeletal muscle mass[22,88]. The nutritive model used in this thesis is ideal due to its unique ability to restrict nutrient availability while avoiding unnecessary stress as seen with intrauterine growth restriction inducing hypoxia or via timed separation of the pups from the mother[89,90].

The type of mouse used in this thesis is the Friend Leukemia Virus B NIH (FVB/N) which is a multipurpose inbred strain purchased from Charles Rivers Laboratory. FVB/N is well known for its ability to produce large litters (an average of 8 or more) and being highly accepting of donor pups from other dams compared to the commonly used C57BL/6J strain[91–93]. Both of these factors allow for ease in utilizing the cross-fostering nutritive model and the capability of reaching a significant sample size in a very short amount of time. Due to consistently using this strain in various projects there is now a large, reproducible index of phenotypic data on growth, body composition, metabolism, skeletal and cardiovascular muscle and function making this the ideal strain for this thesis[6,7,22,88,94].

Metabolomics allows for establishing a ‘metabolic profile’ of the collected tissue, organ or cell and identify biological markers of disease[95–97]. In this thesis we utilize the method of Liquid Chromatography-Tandem Mass Spectrometry (LC-MS/MS) for our metabolomics platform, which

involves separation of molecules by their polarity and mass (more specifically, mass-to-charge ratio), to produce mass spectra. The tandem aspect of the method enables fragmentation of molecules into pieces and measurement of their 'tandem mass spectra' (MS/MS or MS^2). These MS/MS patterns are searched against structure databases to help in their annotation as biological molecules. The LC-MS/MS data in this thesis are analyzed using the Global Natural Products Social Molecular Networking software (GNPS)[95]. Thousands of MS spectra are generated in one set of samples, which would be tedious to analyze and compare to data sets in published data, but the highly efficient algorithms of GNPS and its hosting on the San Diego Supercomputer (SDSC) greatly increases the speed of data analysis. The relative abundance of each metabolite is quantified using mzMine software[98], which is linked to GNPS. Once the data are uploaded on GNPS, the metabolites are identified and labelled according to their signal frequency, molecular weight and chemical structure. Molecular networks are built that help visualize structure similarity in MS/MS fragmentation patters greatly aiding data visualization and analysis. The GNPS platform is used throughout this thesis as a means to detect unique metabolite features, annotate them by comparing to chemical structure databases and globally compare metabolomics profiles between samples.

In summary, many studies have shown promising results towards uncovering mechanisms behind disease onset in the growth restricted population[20,99–101]. The gut microbiome regulates various dynamic metabolic processes in the body and has become an important area of study in understanding human disease[102–104]. There are a few studies showing that there could be a vital connection between the gut microbiome and the growth restricted population[26,76,105], however this area of research is still in its early stages and leaves much to still be uncovered in future work.

INTRODUCTION (Manuscript)

According to the World Health Organization, as of 2018 growth restriction induced by poor nutrition *in utero* and postnatal life affected more than 151 million children globally under the age of 5 years[106]. Growth restricted youth have an elevated risk for chronic disease in adulthood[107–109]. Even with implemented refeeding, the growth restricted population is predisposed to developing cardiovascular disease, type II diabetes, sarcopenia and metabolic syndrome in adulthood[110–112]. Growth restriction and chronic disease are common in poorer nations, making the need for cost-effective interventions a major need to improve global health. In order to develop those treatment strategies, the scientific community needs to better understand the mechanisms behind early life growth restriction and chronic disease in adulthood.

The mammalian gut microbiome is composed of trillions of Bacteria, yeast, phage, and Archaea[52,113–115]. Bacteria that live in the gut contain many different phyla and a multitude of species, many of which are still unknown. Microbes in the gut have myriad functions, some of which are beneficial to the host including, but not limited to, enhancing nutrient absorption, improving digestion, regulating immune responses, as well as altering enzymatic and cell signaling activity in the gut and liver[51,104,116,117]. The gut microbiome has been studied for many years as a potential marker for disease onset as well as a way to prevent or treat certain diseases[13,76,118]. Some studies have even shown remarkable results from transplanting healthy microbes into diseased patients[76,119,120]; although these studies are still in their earlier stages, this sets a strong precedent that the microbiome is nearly another 'organ' that should be continued to be explored to better understand human pathology and disease[113].

The microbiota's fundamental role in human metabolism makes it especially important to the development of disease caused by early life growth restriction[51,121,122]. Microbiome diversity is affected by host genetics, environment, early microbial exposure and diet[52]. The infant gut microbiome is more

variable than adults[53]. At birth, the microbiome is initially highly sensitive to environmental factors[123,124], maternal diet[125–127], gestational age[128] and low birth weight[129]. At approximately 2-3 years of age, the gut microbiome becomes more stable and begins to resemble that of an adult[52]. With the wide variety of external influences that shape the microbiome that occur in early life, it is likely a reduction in nutrient availability would also have lasting effects on the gut microbiome. It has been speculated that the gut microbiome, like other organs and cellular processes, may be stunted in growth restricted individuals[66]. A recent study by Schwarzer *et al.* elucidated potential mechanisms by which the gut microbiome can influence longitudinal growth[26]. When germ free mice were given a specific strain of *Lactobacillus*, growth hormone and insulin-like growth factor (IGF-1) signaling improved, suggesting that certain gut microbes have the ability to induce growth by interacting with the GH-IGF1 axis[13]. Additionally, a separate study by Blanton et al in 2016 showed that when supplementing bacteria from a healthy subject into a growth-restricted subject, their health markers improved, which highlights the gut microbiome as a vital subject to study in this population[76]. Growth restriction induced via undernutrition is associated with various vitamin and nutrient deficiencies, especially B-Vitamins[130–132]. Recent studies suggest that B-Vitamins that are produced by the gut microbiome[126,130] may also play a key role in regulating the GH-IGF-1 axis[133]. Thus, alterations to both the microbial community and the metabolites they produce may alter growth by reducing IGF-1 signaling as well as other potential downstream factors[8–11].

The purpose of this thesis was to determine the composition of the murine gut microbiome and metabolome in both healthy and growth restricted cohorts across the lifespan. We hypothesized that growth restriction induced via undernutrition will significantly alter the microbiome and metabolome across the lifespan compared to healthy controls (CON). Both gestational (GUN) and postnatally (PUN) undernourished mice will be used to elucidate how two different types of growth restriction might affect the microbiome compared to CON. Additionally, we hypothesized growth restriction will lead to decreased muscle and hepatic IGF-1 expression in PUN and GUN mice compared to CON.

METHODS

The present investigation was approved by the Institutional Animal Care and Use Committee at Michigan State University and conducted according to the guide for the care and use of laboratory animals. FVB strain mice were obtained from Charles Rivers Laboratories (Wilmington, MA), and had access to water and food *ad libitum*. Cages were kept in a vivarium maintained at 18-21°C with automatic 12-hour light/dark cycles to minimize stress and optimize environmental conditions.

Nutritive Model

Females were placed onto either a low-protein (LP) diet (8% protein; Research Diets, New Brunswick, NJ, USA) or an isocaloric control diet (CON; 20% protein; Research Diets, New Brunswick, NJ, USA) two weeks prior to breeding. The male mice were then placed into to the female cages for a 24-hour period, allowing all pups to be born at approximately the same time.

At birth, (PN1) pups were pooled, sexed and then dispersed equally to one of three experimental litter groups (4 males, 4 females per litter). Pups were weighed to ensure even distribution and then given a small tattoo on their paw for identification. Control (CON) pups were born from dams fed a 20% protein diet and then reassigned (cross-fostered) to a different dam that was also fed the CON diet. Gestationally undernourished pups (GUN) were growth restricted through feeding the dam the LP diet, and then cross-fostered at PN1 to mothers fed the CON diet. Postnatally undernourished pups (PUN) were born from mothers fed the CON diet during gestation and then cross-fostered at PN1 to dams fed the LP diet. Due to natural occurrences, donor pups were added to maintain litter size, but were not used for further testing in this study. At PN21, all three experimental diet groups were weaned onto the fully nourished CON diet (Fig. 1). Weights were taken twice per week until PN21, and once per week until PN80.

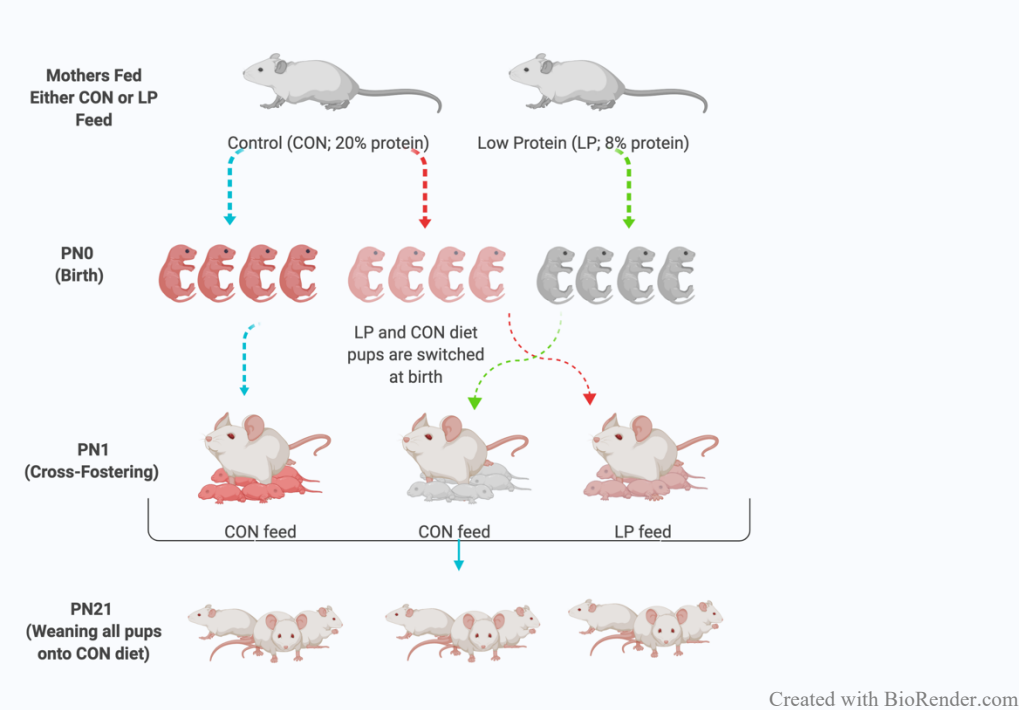

Figure 1: Cross-Fostering Nutritive Model. A nutritive model was created to induce growth restriction during gestation and postnatal life (first 21 days of life, lactation). Females are placed on either a CON or LP diet prior to breeding. At birth (PN1) LP pups are cross-fostered or reassigned to a mother fed the CON diet and vice versa. The CON group is fed the same CON throughout gestation until adulthood (PN80).

Sample Collection

At PN21 and PN80, mice were anesthetized using 1% vaporized isoflurane followed by cervical dislocation. All hindlegs, gastrocnemius, cecum and livers were taken at PN21 and then again in littermates at PN80. The hindlegs were separated from the body and gastrocnemius muscles were surgically removed and placed on dry ice. The remaining tissue was removed from the tibia and then length was measured using Vernier calipers on each leg. Average tibia length was used as a surrogate for body composition and longitudinal growth[134]. After the hindlegs and gastrocnemius were removed, the liver and cecum were then taken out using tweezers sterilized with 70% ethanol and then placed on dry ice. All tissues after dissection were removed from dry ice and placed into the -80°C freezer for later use in western blotting and multi-omics analysis.

Fecal samples were collected from the live mice weekly across the lifespan from PN18-PN80. To collect the sample, the mouse was first placed in a sterile container for up to 5 min. Once a pellet was left in the container, the mouse was returned to its respective cage. The samples were collected using tweezers sterilized with 70% ethanol and placed into a clean centrifuge tube directly on dry ice and stored in the -80°C freezer.

Microbiome Data Generation

Cecum and fecal samples were first diluted with 300 uL of ultra-pure water. Three 2mm steel homogenization beads were added, and the mixture was placed into the Beadruptor at a frequency of 20 Hz for 5 minutes. Then, DNA was isolated from the fecal and cecum samples using the Qiagen Powersoil DNA® extraction kits according to the manufacturer's instructions. Extracted DNA was subjected to PCR amplification of the bacterial 16S rRNA gene targeting the V4 region according to protocols outlined in the Earth Microbiome Project[135]. The amplified DNA were sequenced in the MSU RTSF genomics core on an Illumina® MiSeq® instrument according to their established 16S rRNA Illumina® sequencing pipeline. Quality controlled FASTQ files were demultiplexed and analyzed using the Qiita software[136]. Qiita is based on the Qiime bioinformatics pipeline and includes a deblurring step to identify unique sequences representing different bacterial amplicon sequence variants (ASVs). Microbial physiological functions were outlines for each significant metabolite via established literature in PubMed.

Fecal, Cecum and Liver Metabolomics

Tissue homogenates were extracted in ice cold 70% methanol overnight at 4°C and then pelleted in a benchtop centrifuge at 10,000 x g. Methanol extracts were analyzed by LC-MS/MS mass spectrometry with data dependent fragmentation mode using a Thermo® QExactive mass spectrometer. Briefly, metabolites were separated on a Waters® Aquity® C18-Reverse phase column with a 12 min chromatography run using a LC-MS grade Water: Acetonitrile gradient from 2% to 100%. Eluent was then injected in the mass spectrometer with electrospray ionization and MS^1 and MS^2 spectra captured for 10 mins of the run. During the LC-MS run an internal standard was infused with the extraction solvent (phenol red dye) and a quality control mix of 6 known compounds was injected after every 10 samples. The metabolomics data were converted to the .mzXML format and area-under-curve abundance of each feature was calculated using the mzMine 2 software[98]. The mass spec files were uploaded to GNPS, and library searching and molecular networking were performed using parameters as previously described[95,137]. Metabolic physiological functions were outlines for each significant metabolite via established literature in PubMed.

Western Blot Procedure – Near-Infrared (NIR) Quantification

To evaluate liver and GS for growth factors, a Near-Infrared (NIR) Western blot protocol was utilized, with IGF-1 as the primary target protein. Proteins were extracted with the application of a lysis buffer (composed of 9.9 mL H_20; 0.4 g Chaps, 100 µL Tris 7.5, 1 protease inhibitor pellet) for 15 minutes on ice, followed by Beadruptor tissue homogenization and centrifugation. A Bradford assay[138] was used to determine protein concentration and allow for equal loading of samples onto the SDS PAGE.

Following SDS PAGE electrophoresis, proteins were transferred to PVDF membranes. After protein transfer, the membranes were dried on filter paper at room temperature and then re-wetted with Methanol, followed by the Revert Total Protein Stain reagent (Li-Cor Biosciences). Membranes were

then rinsed in Revert Wash reagent and imaged via ImageStudio software (Li-Cor Biosciences). Then, all membranes were de-stained and then blocked for 1 hour in Intercept Blocking Buffer (Li-Cor). Following the blocking stage, all membranes were incubated with an IGF-1 primary antibody at a 1:2500 ratio (Abcam, Cambridge, Ma) diluted in 5% BSA+TBST overnight at 4°C.

Following overnight incubation, membranes were rinsed in Tris-buffered saline with tween (TBST), and then incubated in 800CW Goat Anti-Rabbit secondary antibody (Li-cor Biosciences) at a 1:15000 ratio for one hour diluted in Intercept Blocking Buffer + 0.01% SDS and 0.02% Tween 20. The membranes were then rinsed again in TBST and then TBS to remove residual Tween 20. Near-Infrared (NIR) images are generated using ImageStudio (Li-cor Biosciences) and analyzed via Empiria (Li-cor Biosciences). Normalized signals for the target protein as well as its respective total protein lane were generated and calculated via Empiria[138–141].

Statistics

For the purpose of this study, the primary hypotheses and aims were focused on determining differences in the microbiome, metabolome, growth markers and IGF-1 between diet groups (GUN, PUN and CON) over time (PN21-PN80). Due to there being no preliminary data on the effect size of growth restriction on -omics data using this mouse model, a reasonable sample size of 5 per diet group and age was chosen as per recommendations suggested in recent reviews of best practices of microbiome and metabolomic study design and analysis[142,143]. A total of 102 mice were generated for this investigation allowing for a cohort of mice evaluated at PN21 (CON Female N=9, CON Male N=9, GUN Female N=7, GUN Male N=7, PUN Female N=7, PUN Male N=5) and PN80 (CON Female N=13, CON Male N=7, GUN Female N=12, GUN Male N=7, PUN Female N=7, PUN Male N=12. Initially, data analysis indicated atypical growth responses for one batch of mice and as such was removed from the analysis. The atypical batch consisted of 37 mice reducing total sample size to 67 mice. Additionally, due to the

unforeseen loss in sample, sexes were pooled in order to yield appropriate sample size for each diet group. The resulting sample size was as follows:

Measurements Across the lifespan (PN18-80):
- Fecal Microbiome/Metabolome: CON N=5, GUN N=6, PUN N=6

PN21 Measurements:
- Growth: CON N=12, GUN N=9, PUN N=7
- IGF-1: CON N=6, GUN N=7, PUN N=5
- Cecum Microbiome/Metabolome: CON N=4, GUN N=6, PUN N=5
- Liver Metabolome: CON N=12, GUN N=6, PUN N=7

PN80 Measurements:
- Growth: CON N=13, GUN N=10, PUN N=12
- IGF-1: CON N=9, GUN N=5, PUN N=8
- Cecum Microbiome/Metabolome: CON N=5, GUN N=6, PUN N=6
- Liver Metabolome: CON N=13, GUN N=9, PUN N=11

Microbiome and metabolome data were both normalized to relative abundance of either total microbial reads (microbiome) or total ion current (metabolome). Microbiome analysis was first performed by analyzing the overall diversity (alpha-diversity) between diet groups in Qiita. Faith's Index of Phylogenetic Diversity (FD) was used to test the alpha-diversity of the microbiome between GUN, PUN and CON groups using a Kruskal-Wallis and post-hoc Wilcoxon Rank-Sum Test in Qiita. Beta-diversity was evaluated using data from taxonomic level 7 (ASV-7). The weighted UniFrac distance was calculated between all samples and Permutational Multivariate Analysis of Variance (PERMANOVA) was used to test for statistically significant clustering by treatment group using the microbial 16S rRNA gene sequences of each sample at each time point. Beta-diversity was visualized by projecting the distance matrix in 3 dimensions using Principal Coordinate Analysis Plots (PCoA plot) in Emperor. The dissimilarity and distance matrices used to create the PCoA plot allow one to see similarities (clustering) and differences (separation) between each sample. To further identify and evaluate the taxonomic profile of the microbiome between treatment groups, the data was extracted from Qiita and a Random Forest (RF) machine learning classification algorithm was run in R-Studio with the randomForest package to determine the strength of different sample characteristics on the overall microbiome data. This model was

run with 5000 trees and no set seed. Out-of-bag error rates were used to assess overall model classification strength and Variable Importance Plots (VIP) were generated to identify the strongest classifiers. The VIP, in this case, is a list of microbes that are assigned a score of Mean Decrease Accuracy (MDA) for its contribution to the classification. The VIP is then sorted from highest to lowest in excel and a raw metadata list of the microbes is created. There are currently no foundational guidelines set for how low of an MDA score is worth analyzing, however, for the purposes of this thesis and to eliminate false positives, a minimum MDA of 5.0 was used. The microbial relative abundances were then subjected to linear mixed model analysis (LMM) in SAS comparing treatment groups with time as a covariate. A Bonferroni's Correction for p-value was used to lower false discovery rate and any remaining microbes were then used for further analysis (fecal alpha level <0.0015; cecum alpha level <0.0005). Further longitudinal analysis was performed on the statistically significant microbes via linear regression and Analysis of Covariance (ANCOVA) of slope differences between treatment groups with time (in weeks) as a covariate (alpha 0.05).

Metabolomics statistical analysis was performed using a Bray-Curtis distance metric instead of the UniFrac distance since it is solely a phylogenetic-based metric. Once the metadata list of metabolites from the VIP was generated, the data was then normalized to total abundance for each metabolite and ran in SAS, where it was log transformed then subjected to LMM testing (alpha 0.05). For the liver data, that did not contain a linear time component, differences between treatment groups were tested with a Kruskal-Wallis test and post-hoc Wilcoxon-rank sum tests at either PN21 or PN80.

Phenotypic growth markers (body weight, muscle weight, tibia length) were standardized to total body weight and analyzed using repeated measures ANOVA to analyze differences between treatment groups in JMP Pro 14.0 (alpha 0.05) and a 2-way ANOVA and subsequent post-hoc Tukey's to examine differences at each time point.

RESULTS

Evaluation of Phenotypic Markers of Growth

Longitudinal Growth Rate Analysis

Longitudinal body weight analyses (Fig. 2) was performed via a repeated measures ANOVA showing an overall diet effect ($p<0.001$). Post-hoc Tukey's analysis revealed that PUN mice were overall significantly lower in body weight over time compared to GUN and CON ($p<0.001$). GUN was not overall significantly smaller over time compared to CON, however, a secondary 2-way ANOVA and post-hoc Tukey's revealed significant changes in body weight at specific timepoints. GUN was initially

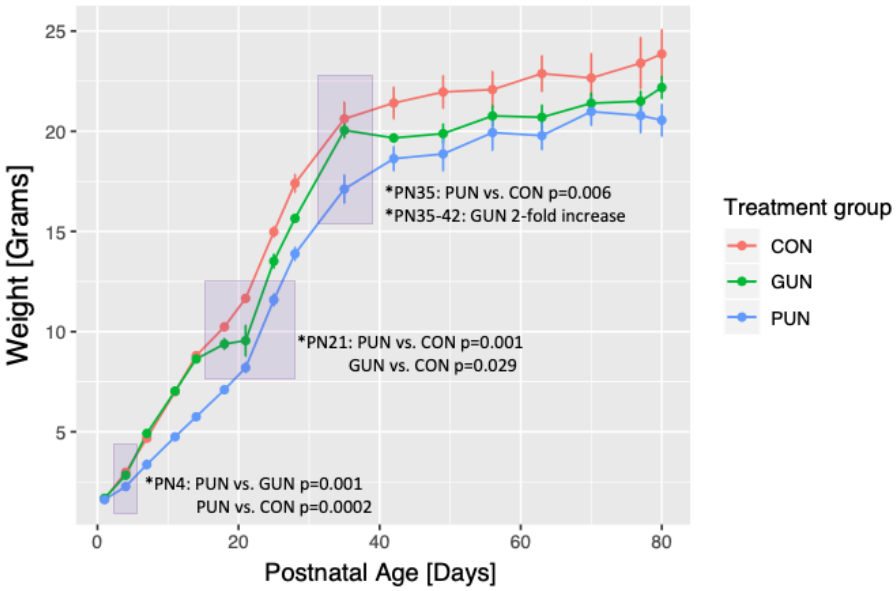

Figure 2: Growth of PUN, GUN and CON mice from birth (PN1) to adulthood (PN80). Longitudinal body weight analysis from PN1-PN80 of CON (n=25), GUN (n=19), and PUN (n=19) mice via a repeated measures ANOVA resulted in an overall diet effect ($p<0.001$). Post-hoc Tukey's analysis revealed that PUN mice were significantly lower in body weight across the lifespan ($p<0.001$). There was no overall difference between GUN and CON over time, however, a 2-way ANOVA and post-hoc Tukey's was also performed to examine differences at each time point, which revealed a distinct decrease in weight of PUN from GUN and CON at PN4, which remained lower until adulthood (PN80). GUN mice remained similar in weight to CON from PN1-PN14, decreases in weight from PN18-28, and then subsequently spikes in weight from PN35-42 (2-fold increase), and finally normalizes to CON weights until PN80.

similar to CON from PN1-PN14, and then significantly decreased from PN18-PN28 (p=0.029). After PN28, GUN experienced an increase in weight gain (2-fold increase from PN35 to PN42) which then normalized to similar weights to CON from PN35-PN80. Additionally, PUN was initially a similar weight at PN1 to the other diet groups, but then was significantly lower than GUN (p=0.001) and CON (p=0.0002) at PN4 and continued to stay significantly lower until PN80.

Gastrocnemius (GS) weights were also analyzed with a 2-way ANOVA and post-hoc Tukey's (fig. 3), revealing a significant diet effect (p=0.0008), showing CON GS were overall larger than GUN (p=0.007) and PUN (p=0.037) over time. Tibia lengths and liver weights were also analyzed and resulted in overall age effects (p<0.001) with tibias (p<0.001) and livers (<0.001) at PN21 being significantly smaller than at PN80. Tibias and livers were not significantly different between diet groups. There were no other diet or diet*age effects found.

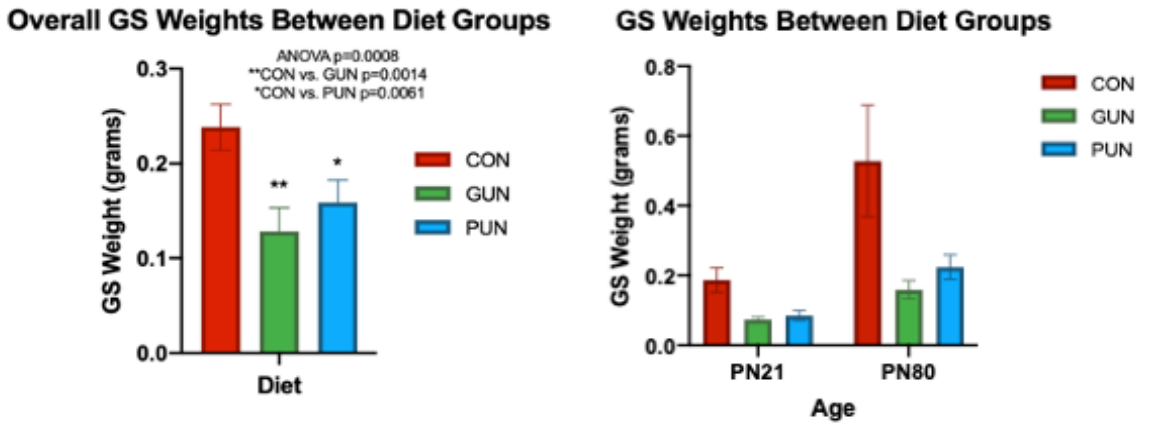

Figure 3: Overall Comparison of GS weights between PUN, GUN and CON mice at PN21 and PN80. Gastrocnemius (GS) weights were also analyzed with a 2-way ANOVA and post-hoc Tukey's (PN21: CON n=12, GUN n=9, PUN n=7; PN80: CON n=13, GUN n=10, PUN n=12) revealing a significant overall diet effect (p=0.0008) with CON GS being primarily overall larger than GUN (p=0.0014) and PUN (p=0.0061). There was a significant age effect found (p<0.0001) showing that GS were overall larger at PN80 within treatment groups, however this is to be expected. There were no significant age*diet effects found.

Western Blot Analyses of Hepatic and Muscular IGF-1 Expression

NIR Total Protein Stain Western blot (WB) data, analyzed via a 2-way ANOVA, revealed an overall diet*age effect (p=0.0005) in liver IGF-1, further analyzed via a post-hoc Tukey's test, which showed significantly low expression of PUN (p<0.001) and GUN (p=0.0012) at PN21 compared to CON (Fig. 4). PUN trended lower in hepatic IGF-1 expression in comparison to GUN at PN21 but the values were not significantly different (p>0.05). Additionally, there was a significant overall age effect showing liver IGF-1 was expressed less at PN80 versus PN21 (p=0.0002). There were no differences found between diet groups at PN80.

In addition to testing liver samples, IGF-1 was also tested via WB in the gastrocnemius muscle (GS) between diet groups over time, which revealed an overall deficit of expression in PUN (p=0.037) and GUN (p=0.007) compared to CON. There was no significant age effect found in the GS (Fig. 5).

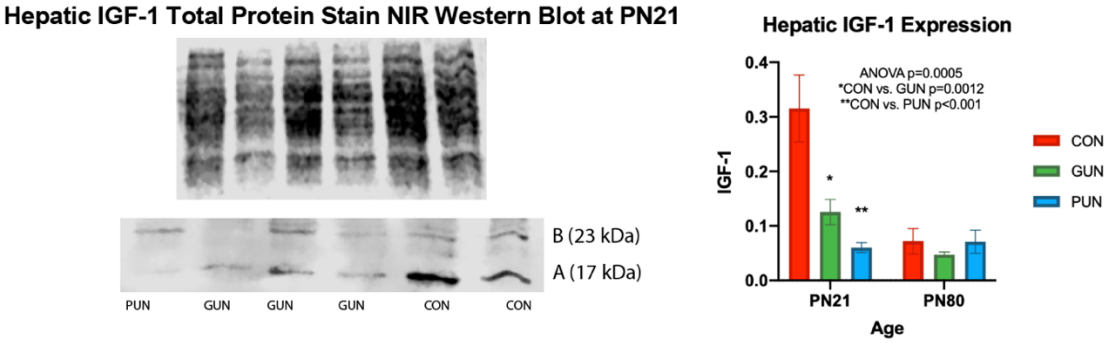

Figure 4: Hepatic IGF-1 Expression in PUN, GUN and CON mice at PN21 and PN80. Hepatic IGF-1 was analyzed via a 2-way ANOVA and post-hoc Tukey's test at PN21 (CON n=6, GUN n=7, PUN n=5) and PN80 (CON n=9, GUN n=5, PUN n=8). The ANOVA resulted in an overall significant difference between diet groups over time (p=0.0005). Post-hoc test results revealed a significant decrease in PUN (p<0.001) and GUN (p=0.0012) Liver IGF-1 expression compared to CON at PN21. Signals were quantified from a sum of two IGF-1 isoforms: IGF-1A (17 kDa) and IGF-1B (23 kDa) to represent total IGF-1 expression. There was a significant overall age effect showing liver IGF-1 was expressed less at PN80 versus PN21 (p=0.0002). There were no significant diet effects found at PN80, thus the represented blot shown above is from PN21. The histogram (right) represents the overall normalized signal expression in each diet group. The error bars are representative of standard error.

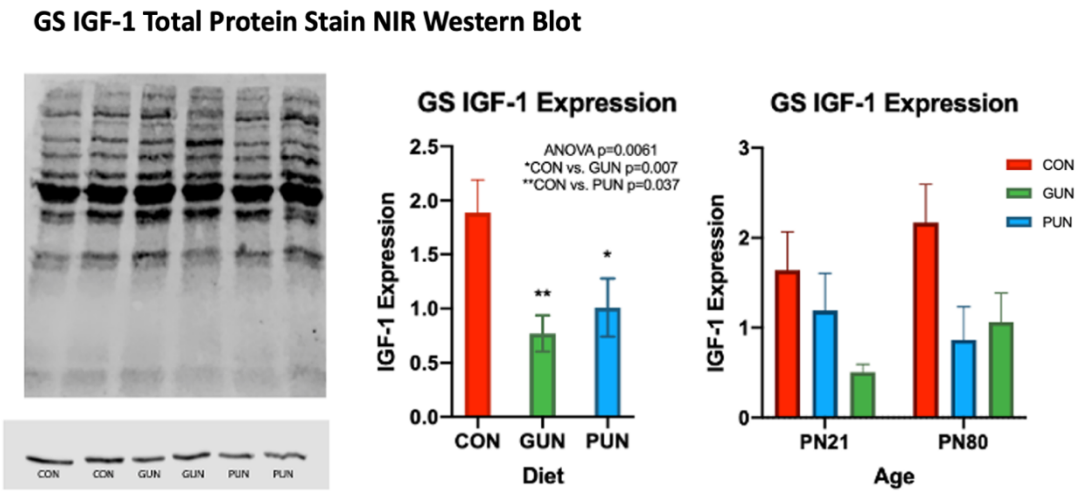

Figure 5: IGF-1 Expression in GS muscle in PUN, GUN and CON mice. IGF-1 signal was analyzed via a 2-way ANOVA (PN21: CON n=6, GUN n=7, PUN n=5; PN80: CON n=9, GUN n=5, PUN n=8) which revealed an overall diet effect (p=0.0061). Post-hoc Tukey's analysis showed a significant decrease in IGF-1 expression in PUN (p=0.037) and GUN (p=0.007) GS compared to CON. There was no significant diet*age effect found, thus PN21 and PN80 were combined in the graph and blot shown above. Additionally, only one isoform of IGF-1 was found in the GS samples as compared to the liver (IGF-1A; kDa 17). The histogram (right) represents the overall normalized signal expression in each diet group. The error bars are representative of standard error.

Fecal Microbiome – Alpha-Diversity

Analysis of Multi-Omics Data from Fecal Samples

Using a linear mixed-effects model with time (in weeks) as a covariate, the overall phylogenetic alpha-diversity of the microbiome of the fecal samples was highest in the PUN group (p=0.011) compared to GUN and CON from weeks 1 through 5 (Fig. 6). The GUN group had the second highest alpha-diversity but was not significantly different compared to CON (p=0.07). To determine alterations in alpha-diversity over the lifespan, a linear regression was used, and slopes were calculated, resulting in CON (m=0.83) having the largest increase in alpha-diversity over time, followed by PUN (m=0.31) and GUN (m=0.29). A secondary ANCOVA test, which compares slopes, confirmed PUN was significantly

different from CON (ANCOVA p=0.0028, Tukey's HSD PUN-CON p=0.036). There was no significant difference found in slopes between PUN and GUN.

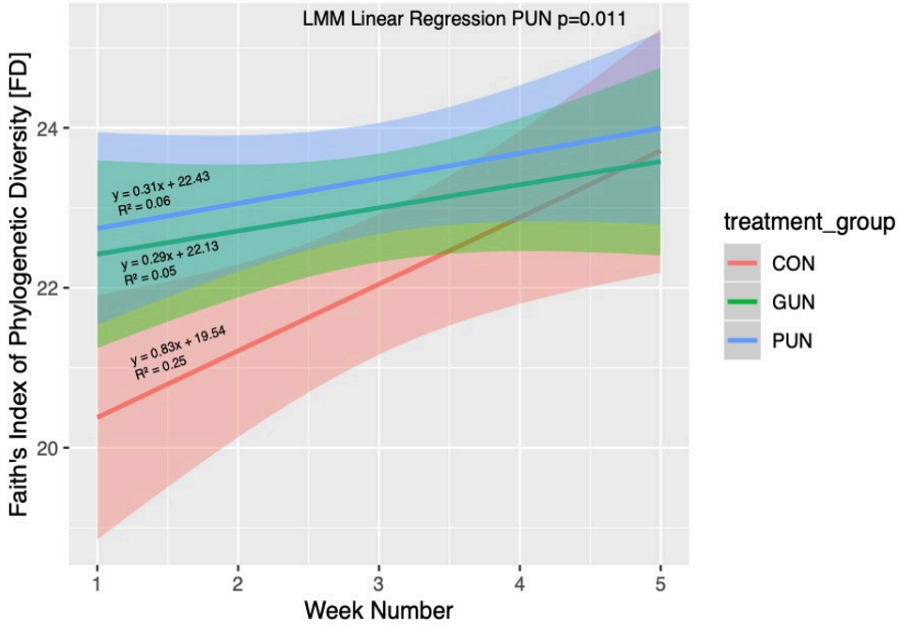

Figure 6: Alpha-Diversity of Fecal Samples from weeks 1-5. Linear regression analysis of the Faith's Phylogenetic diversity (FD) through weeks 1-5 with LMM (overall treatment group differences) and ANCOVA test results (slope differences). PUN had the highest alpha-diversity over time (p=0.011) and the PUN and CON slopes were different from each other (p=0.036). Shaded colors in the plot represent the 95% confidence intervals with the main colored line being the mean FD for each diet group. The slope for each group is as follows: PUN (m=0.31), GUN (m=0.29), CON (m=0.83), which shows there is the strongest increase in diversity over time in CON compared to GUN and PUN, which changed little through time.

Fecal Microbiome – Beta Diversity

Beta-diversity analysis compared microbiome profile differences between CON, GUN and PUN from weeks 1 through 5 by calculating the UniFrac distances and testing for clustering by groups using a PERMANOVA test. All three diet groups were found to be significantly different from each other (Fig. 4: p=0.001). The pseudo-F for the pairwise comparison of PUN and CON was shown to be the highest (20.39) was the highest compared to other pairwise comparisons tested followed by PUN and GUN

(18.86). The low pseudo-F value between CON and GUN (2.84) indicates there are very few differences between their beta-diversities. The beta-diversity relationships were visualized using a PCoA plot (Fig. 7).

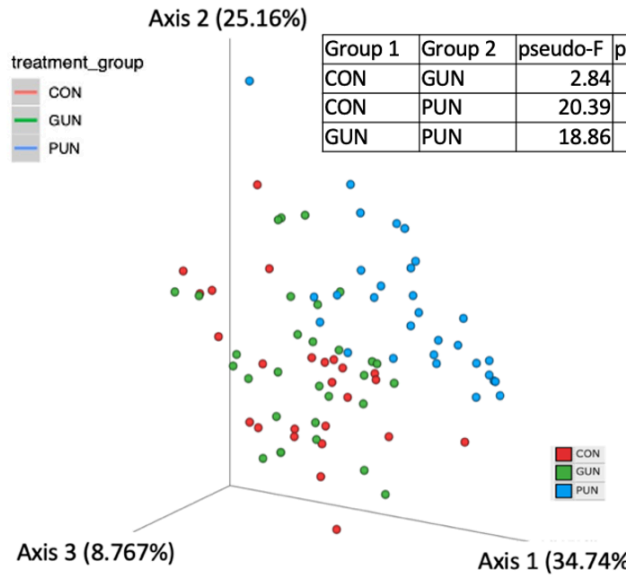

Group 1	Group 2	pseudo-F	p-value	q-value
CON	GUN	2.84	0.032	0.032
CON	PUN	20.39	0.001	0.0015
GUN	PUN	18.86	0.001	0.0015

Figure 7: Weighted UniFrac PCoA Plot of Fecal Microbiome. PCoA analysis of the Weighted UniFrac distances between CON (n=25), GUN (n=30), and PUN (n=30) from weeks 1-5 displayed significant differences, via separation and subsequent clustering of samples between all three diet groups (PERMANOVA; p=0.001) over time. The table shows the pairwise statistical comparisons. The pseudo-F value between PUN and CON (20.39) was the highest compared to other pairwise comparisons tested, indicating these two groups having the strongest differences.

To further identify bacterial OTUs that contribute most to between treatment groups, a random forests (RF) machine-learning classification was run on the treatment group variable, testing how closely the microbiome data reflected the treatment categories category (PUN, GUN, or CON). The out-of-bag error rate (OOB) of the RF model found strong classification between treatment groups (OOB: 14.1%; Fig. 5) indicating robust grouping of treatment groups based on the microbial profiles. The classification was especially strong for the PUN group, with 0% error rate, while CON and GUN had higher error rates (CON: 0.32%; GUN: 0.13%; Table within Fig. 7). The variable Importance Plot (VIP; Fig. 8) listed the most significantly different microbes between diet groups, as denoted by mean decrease accuracy (MDA; higher indicates stronger level of differences). To eliminate false discovery rate, the minimum MDA used

for further analysis was set to a minimum score of 5.0. A Bonferroni's Correction for p-value (alpha <0.0015) was used to filter the LMM results from this list, leading to the top 6 microbes (Fig. 9)

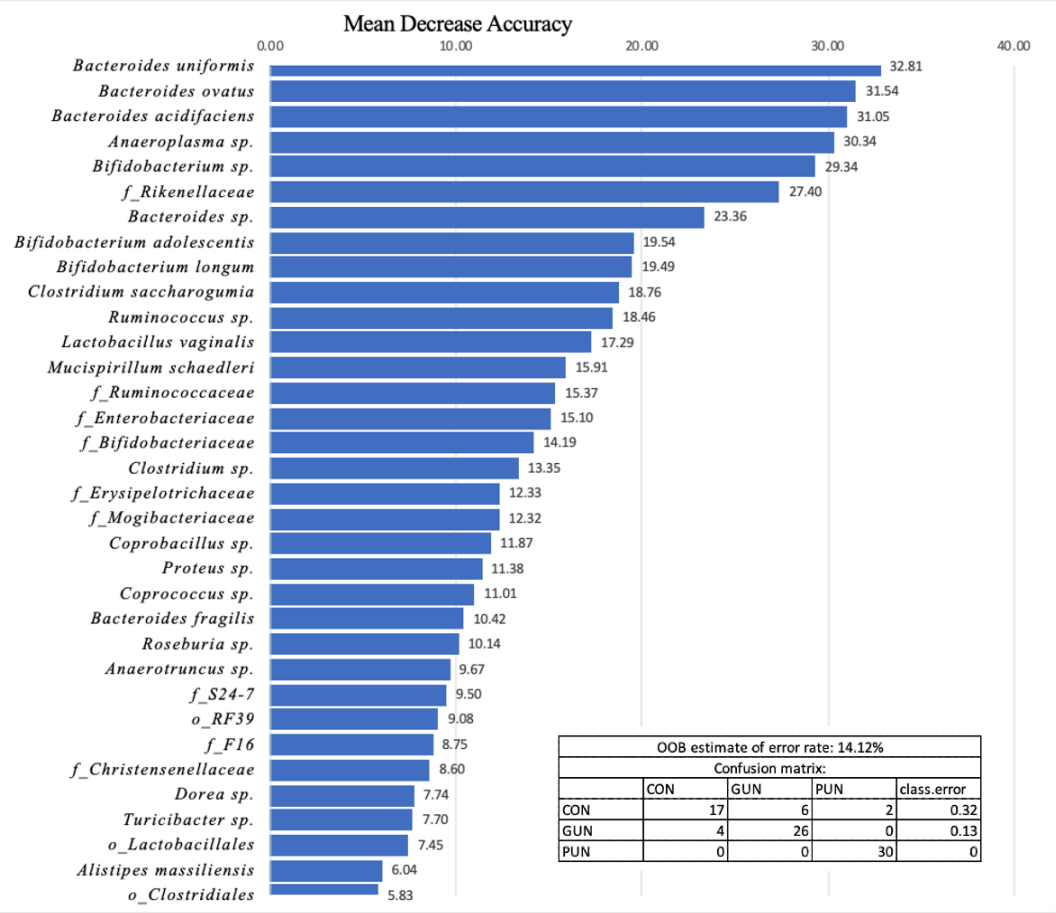

Figure 8: Microbiome Taxonomic Analysis – Variable Importance Plot. The taxonomic analysis via RF revealed the top 45 most diverse fecal microbes in fecal samples collected in CON (n=25), GUN (n=30), and PUN (n=30) mice from weeks 1 through 5 (sample size in mice: CON (n=5), GUN (n=6), and PUN (n=6) mice with 5 samples collected per mouse). In order to limit false discovery rate, the minimum MDA used for further analysis was set to 5.0. A Bonferroni's Correction for p-value (alpha <0.0015) was used to filter the LMM results from this list, leading to the top 6 microbes (Fig. 6). An OOB error classification is shown in the confusion matrix in the lower right (14.12%).

Individual Microbe Changes Between Treatment Groups and Through Time

LMM analysis of fecal samples across the lifespan revealed PUN having a significantly higher abundance of specific bacteria compared to GUN and CON over time including: *Bacteroides uniformis* ($p=2.46\ e^{-14}$), *B. acidifaciens* ($p=2e^{-16}$), *B. ovatus* ($p=2.81e^{-14}$), *Bifidobacterium sp.* ($p=4.81e^{-05}$), and *Clostridium sacchrogumia* ($p=1.96e^{-05}$). An amplified sequence variant belonging to the family Rikenellaceae (f_Rikenellaceae, $p=8.21e^{-13}$) was the only microbe that was significantly lower in abundance in the PUN group over time compared to GUN and CON. These microbes were not significant between GUN and CON over time (Fig. 9). Additionally, there were no microbes present that were

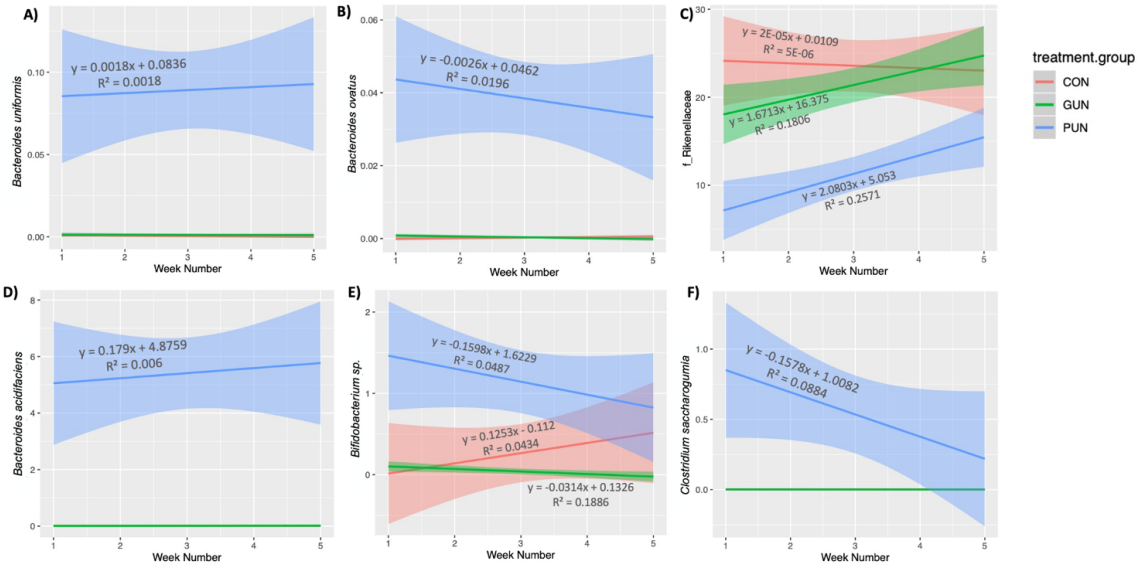

Figure 9: Linear regression analysis of normalized abundance of bacterial operational taxonomic units (OTUs). Bacterial abundances were analyzed using a linear regression over time (weeks 1-5) in CON (n=5), GUN (n=6), and PUN (n=6) mice. The PUN diet group had a significantly higher abundance of *Bacteroides uniformis* (A, $p=2.46\ e^{-14}$), *Bacteroides ovatus* (B, $p=2.81\ e^{-14}$), *Bacteroides acidifaciens* (D, $p<2.0\ e^{-16}$), *Bifidobacterium sp.* (E, $p=4.81\ e^{-05}$) and *Clostridium saccharogumia* (F, $p=1.96\ e^{-05}$) as compared to CON and GUN. Rikenellaceae was the only microbe that showed a significantly low abundance in the PUN group vs. CON and GUN (C, $p=8.21\ e^{-13}$). No significant differences were found between GUN and CON over time. Shaded colors in the plot represent the 95% confidence intervals with the main colored line being the mean microbial abundance for each diet group.

significantly different between the CON group only compared to PUN and GUN and vise versa. The majority of bacterial species found were carbohydrate fermenters and did not recover in adulthood (Table 1).

Table 1: Fecal Microbial Analysis between PUN, GUN, and CON over weeks 1 through 5.

Microbes	*Recovered(Y/N)*	*Physiological Relevance*
B. uniformis	N	Degrades flavonoids; highest glycolytic fermenting capacity compared to other *Bacteroides* species*;* Has been shown to improve insulin sensitivity; Bile-resistant; produces acetic, lactic, and propionic acids; produces bile salt hydrolase
B. acidifaciens	N	Carbohydrate fermenter; Degrades flavonoids; Bile-resistant; produces acetic, lactic, and propionic acids; produces bile salt hydrolase
B. ovatus	N	Carbohydrate fermenter; Degrades flavonoids; Bile-resistant; produces acetic, lactic, and propionic acids; produces bile salt hydrolase
Bifidobacterium sp.	N	Carbohydrate fermenter – primarily sugars in breastmilk; Most abundant in postnatal life; Seen in low but static abundance in adult healthy subjects
C. saccharogumia	N	Converts plant ligands via fermentation into phytoestrogens: Enterodiol and Enterolactone
f_Rikenellaceae	N	Related to *Bacteroides* but is bile-resistant; associated with leptin-resistance, obesity and type 2 diabetes

Fecal Microbe data was further analyzed to determine the recovery rate of microbial abundance into adulthood (week 5), which revealed undernutrition induced growth restriction caused permanent disruption to the PUN gut microbiome from young adolescence (week 1) into adulthood.

Cecum Microbiome – Alpha-Diversity

A LMM of the cecum samples revealed a significantly lower alpha-diversity at PN21 in each diet group which recovered at PN80 (p=0.0112; Fig. 10), this was only observed within the treatment group itself (i.e. PUN at PN21 vs. PUN at PN80) between each diet group over time.

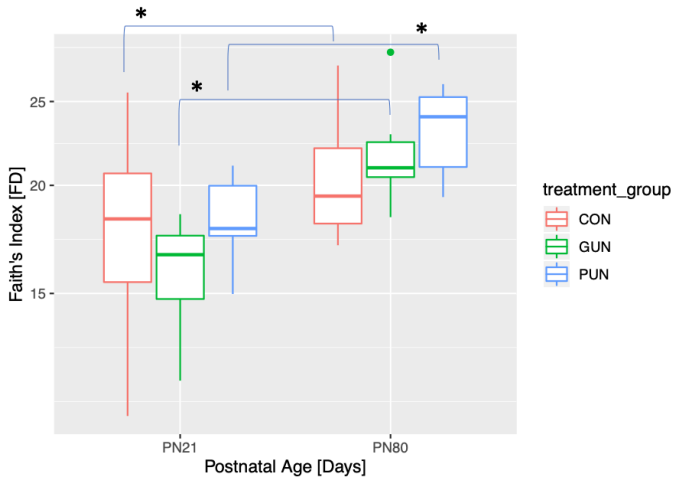

Figure 10: Cecum Alpha-Diversity Faith's Phylogenetic Diversity Metric. LMM testing of the cecum samples in each diet at PN21 (CON n=4, GUN n=6 and PUN n=5) and PN80 (CON n=5, GUN n=6 and PUN n=6) revealed significantly lower alpha-diversity at PN21 in each treatment group that increases at PN80 (*PN21 vs. PN80: p=0.0112). No significant differences were found between diet groups over time.

Cecum Microbiome – Beta-diversity

A PERMANOVA test on treatment group was run against the weighted UniFrac distances between samples collected at PN21 and PN80, due to the significant changes in the microbiome observed between these dates. The PUN group had significantly different beta-diversity at PN21 (p=0.005; pseudo-F=10.65) and PN80 (p=0.012; pseudo-F=2.69) compared to CON and GUN (p=0.005; pseudo-F=10.65) and also at PN80 (p=0.012; pseudo-F=2.69). PUN had significantly different beta-diversity from GUN at

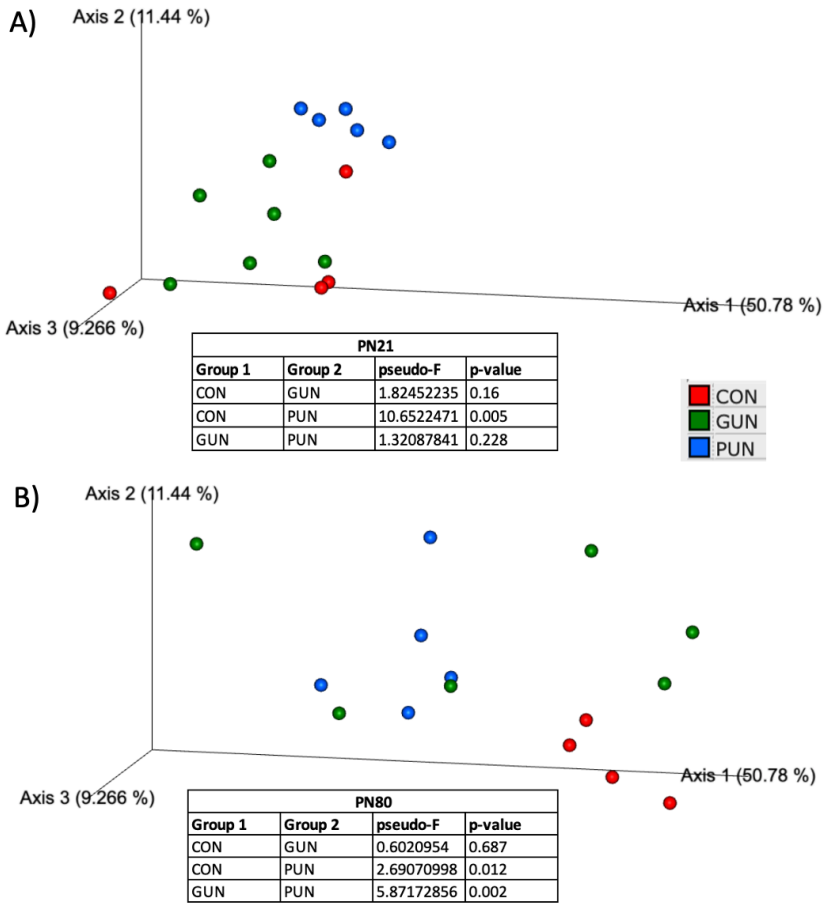

PN21			
Group 1	Group 2	pseudo-F	p-value
CON	GUN	1.82452235	0.16
CON	PUN	10.6522471	0.005
GUN	PUN	1.32087841	0.228

PN80			
Group 1	Group 2	pseudo-F	p-value
CON	GUN	0.6020954	0.687
CON	PUN	2.69070998	0.012
GUN	PUN	5.87172856	0.002

Figure 11: Cecum Microbiome Beta-diversity - Weighted UniFrac. This PCoA is displaying the entire cecum data set over two time points, at PN21 [11A; PUN (n=5), GUN (n=6), CON (n=4)] and then at PN80 [11B; PUN (n=6), GUN (n=6), CON (n=5)]. Significant differences in Beta-diversity were found between CON and PUN at PN21 (p=0.005) and also at PN80 (p=0.012) as well as between PUN and GUN at PN80 (p=0.002). No significant differences were found between GUN and CON over time.

PN80 (p=0.002; pseudo-F=5.871). No significant differences were found between GUN and CON over time (Fig. 11). A RF model was then generated on PN21 and PN80 separately, and a VIP was created of microbes with an MDA of 5.0 or higher with a Bonferoni correction for alpha level set at 0.001 to eliminate possibility of false discovery, leaving three primary microbes seen in Fig. 11 below.

Individual Cecal Microbe Changes Between Treatment Groups Over Time

Cecum taxonomic analysis showed significantly decreased abundance in Rikenellaceae in PUN (p=0.004) at PN21 compared to CON. Rikenellaceae remained lower in PUN compared to GUN and CON at PN80, although this finding was not statistically significant. At PN80, *B. acidifaciens* (p=0.0003), and *B. uniformis* (p=0.0005) were significantly higher in abundance compared to CON (Fig. 13/Table 2). All statistically significant microbes found in the cecum taxonomic analysis reflected those found in the fecal samples, in that there was higher sugar-fermenting *Bacteroides* and lower Rikenellaceae in PUN compared to GUN and CON. These microbes aside from Rikenellaceae remained different from CON through adulthood (Table 2).

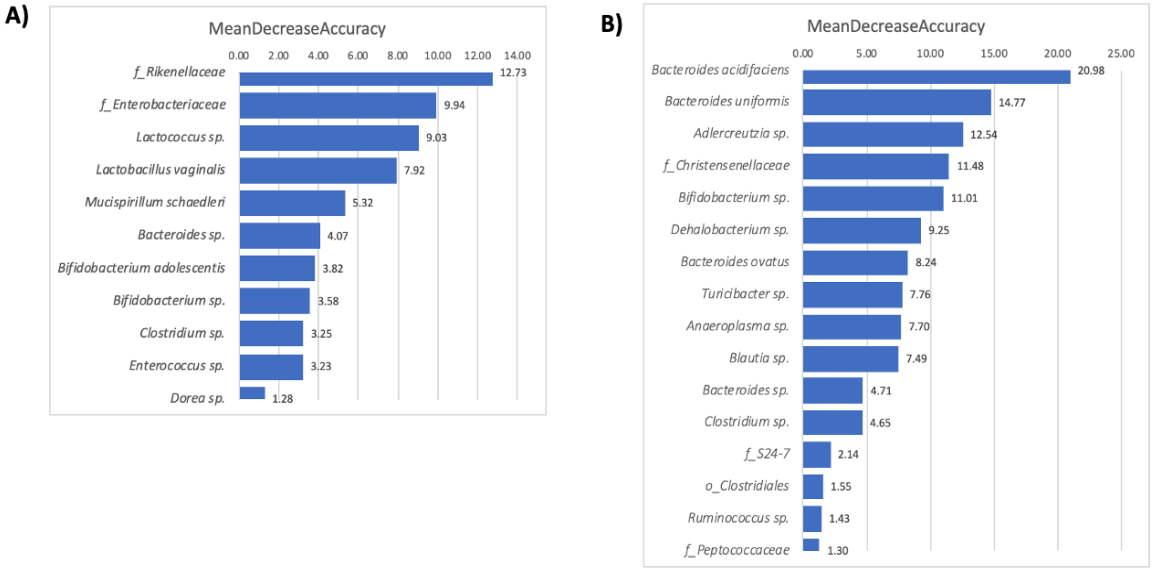

Figure 12: VarImp Plot of Cecum Samples at PN21. Taxonomic analysis for the cecum samples followed the same protocol as mentioned prior but instead only tested timepoints PN21 (Fig. 9A), and PN80 (Fig. 9B) to avoid euthanizing more than necessary in order to collect samples. The majority of microbes listed in the cecum samples were replicates from the ones found in the fecal samples denoting interesting similarities between fecal and cecum microbial abundances.

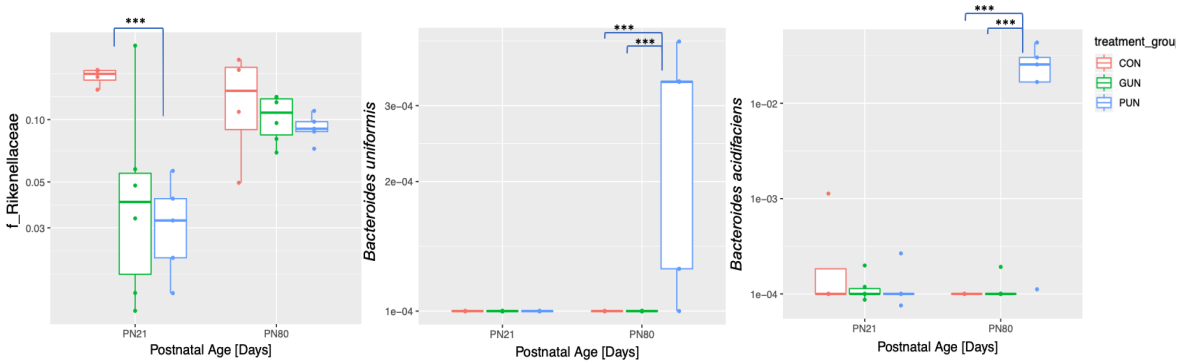

Figure 13: Microbial Boxplots of Cecum Samples between CON, GUN and PUN from PN21 and PN80. Postnatal undernutrition caused significantly increased abundance of *B. acidifaciens* (p=0.0003), and *B. uniformis* (p=0.0005) compared to CON at PN80. The primary microbial difference observed at PN21 that recovered at PN80 was a significant decrease in Rikenellaceae in PUN (p=0.004) compared to CON. (p-value notation: *<0.05, **<0.01, ***<0.0001.

Table 2: Cecum Microbes between PUN, GUN, and CON at PN21 and PN80.

Cecum Microbes	*Recovered(Y/N)*	*Physiological Relevance*
B. acidifaciens	N	Ferments carbohydrate into SCFAs; Bile-resistant; produces bile salt hydrolase
B. *uniformis*	N	Ferments carbohydrate into SCFAs; Bile-resistant; produces bile salt hydrolase
f_Rikenellaceae	Y	Related to *Bacteroides* but is bile-resistant; associated with leptin-resistance, obesity and type 2 diabetes

Analysis of this data set revealed microbes that were overall significantly affected by undernutrition across the lifespan and did not recover in adulthood: B. acidifaciens (PUN p=5.32 E-05), and B. uniformis (PUN p=0.0016) compared to CON. Rikenellaceae was significantly decreased in PUN (p=0.0036) compared to CON.

Liver Metabolomics

A random forest classification model was built on treatment group for both the PN21 and PN80 metabolomic data separately. Neither dataset showed strong overall signatures by treatment group (error rate PN21=41.38%, error rate PN80 = 51.43%). However, the VIP plots from these models still identified known metabolites separating the two groups.

Majority of liver metabolites were significantly affected by postnatal growth restriction (PUN) as compared to gestational growth restriction (GUN). PUN had abnormal deficits compared to CON at PN21 in Cholic Acid ($p=0.001$), Muricholic Acid ($p<0.001$), Glycocholic Acid ($p=0.03$), Taurocholic Acid ($p=0.0079$), Riboflavin ($p=0.003$), and Total EAAs: Methionine ($p=0.0018$), Phenylalanine ($p=0.0015$), and Tyrosine ($p=0.0041$). Two other EAAs, Histidine and Tryptophan were notably low in PUN at PN21, but the differences were not significant between treatment groups ($p>0.05$).

Alternatively, PUN had abnormally high levels of Oleoyl L-Carnitine (also known as Oleoyl carnitine; $p=0.0038$), Palmitoyl carnitine ($p=0.0096$) and Biliverdin ($p=0.020$), but these recovered at PN80. Corticosterone was the only metabolite to be significantly increased in abundance in GUN compared to PUN and CON at PN21 ($p=0.043$). Dehydroepiandrosterone (DHEA) abundance was not present in any diet groups at PN21 due to it not being endogenously produced yet. DHEA remained significantly low in PUN at PN80 compared to GUN and CON ($p=0.018$); (Fig. 14; Table 3). In light of the strong bile acid signatures, the total bile acids in the entire dataset were summed and compared, showing that PUN and GUN had decreased total bile acids in the liver ($p=0.0064$, $p=0.034$, respectively).

Table 3: Liver Metabolites between PUN, GUN, and CON at PN21 and PN80.

Metabolite	*Recovered(Y/N)*	*Physiological Relevance*
Cholic Acid	Y	Energy homeostasis – regulator of glucose and fat metabolism through Farnesoid X Receptor (FXR) and G-protein-coupled bile acid receptor (TRG5) activity
Muricholic Acid	Y	Regulates fat and glucose metabolic activity through FXR and TRG5 receptors; Can also bind to taurine to inhibit FXR activity
Glycocholic Acid	Y	Glycine conjugated form of cholic acid; Downregulation results in inability to digest and absorb fat into the cell for storage/energy resulting in digestive abnormalities;
Taurocholic Acid	Y	Taurine conjugated form of cholic acid; Downregulation results in inability to digest and absorb fat into the cell for storage/energy resulting in digestive abnormalities;
Corticosterone	Y	Induces premature differentiation of GH releasing cells and IGF1-BP; Overabundance leads to protein degradation
Biliverdin	N	Precursor metabolite of Bilirubin, which was also notably high in PUN ($p>0.05$) compared to GUN and CON; Abnormally high biliverdin and bilirubin signifies liver inflammation and liver disease development due to its injurious effects on hepatocytes
L-Kynurenine	Y	Tryptophan metabolite;
Total Methionine	Y	Start codon for tissue growth and protein synthesis; regulates metabolism and mitochondrial ROS production;
Total Phenylalanine	Y	EAA necessary for protein synthesis; Precursor to tyrosine; plays an integral role in the structure and function of proteins and enzymes and the production of other amino acids
Total Tyrosine	Y	Non-essential amino acid; synthesized from phenylalanine; necessary for protein synthesis
Oleoyl L-Carnitine	Y	Oleoyl carnitine is a long-chain acylcarnitine that accumulates during certain metabolic conditions, such as fasting;
Palmitoyl carnitine	Y	Ester derivative of carnitine (long-chain acylcarnitine) involved in the metabolism of fatty acids;
DHEA	N	Endogenous adrenal androgen hormone that regulates IGF-1 circulation and muscle hypertrophy; has protective effects against insulin resistance, cardiovascular disease and cancer

Majority of liver metabolites were significantly affected by postnatal growth restriction (PUN) as compared to gestational growth restriction (GUN). PUN had abnormal deficits compared to CON at PN21 in Cholic Acid ($p=0.001$), Muricholic Acid ($p<0.001$), Glycocholic Acid ($p=0.03$), Taurocholic Acid ($p=0.0079$), Total Bile Acids (sum of primary and secondary; $p=0.0064$), Riboflavin ($p=0.003$), and Total EAAs: Methionine ($p=0.0018$), Phenylalanine ($p=0.0015$), and Tyrosine ($p=0.0041$). Two other EAAs, Histidine and Tryptophan were notably low in PUN at PN21, but the differences were not significant between treatment groups ($p>0.05$). Alternatively, PUN had abnormally high levels of Oleoyl L-Carnitine ($p=0.0038$) and Palmitoyl carnitine ($p=0.0096$) and Biliverdin ($p=0.020$), but these recovered at PN80. GUN at PN21 had abnormally low total bile acids ($p=0.0384$) compared to CON and abnormally high Corticosterone compared to PUN ($p=0.04$) and CON ($p=0.043$). DHEA remained significantly low in PUN at PN80 compared to GUN and CON ($p=0.018$).

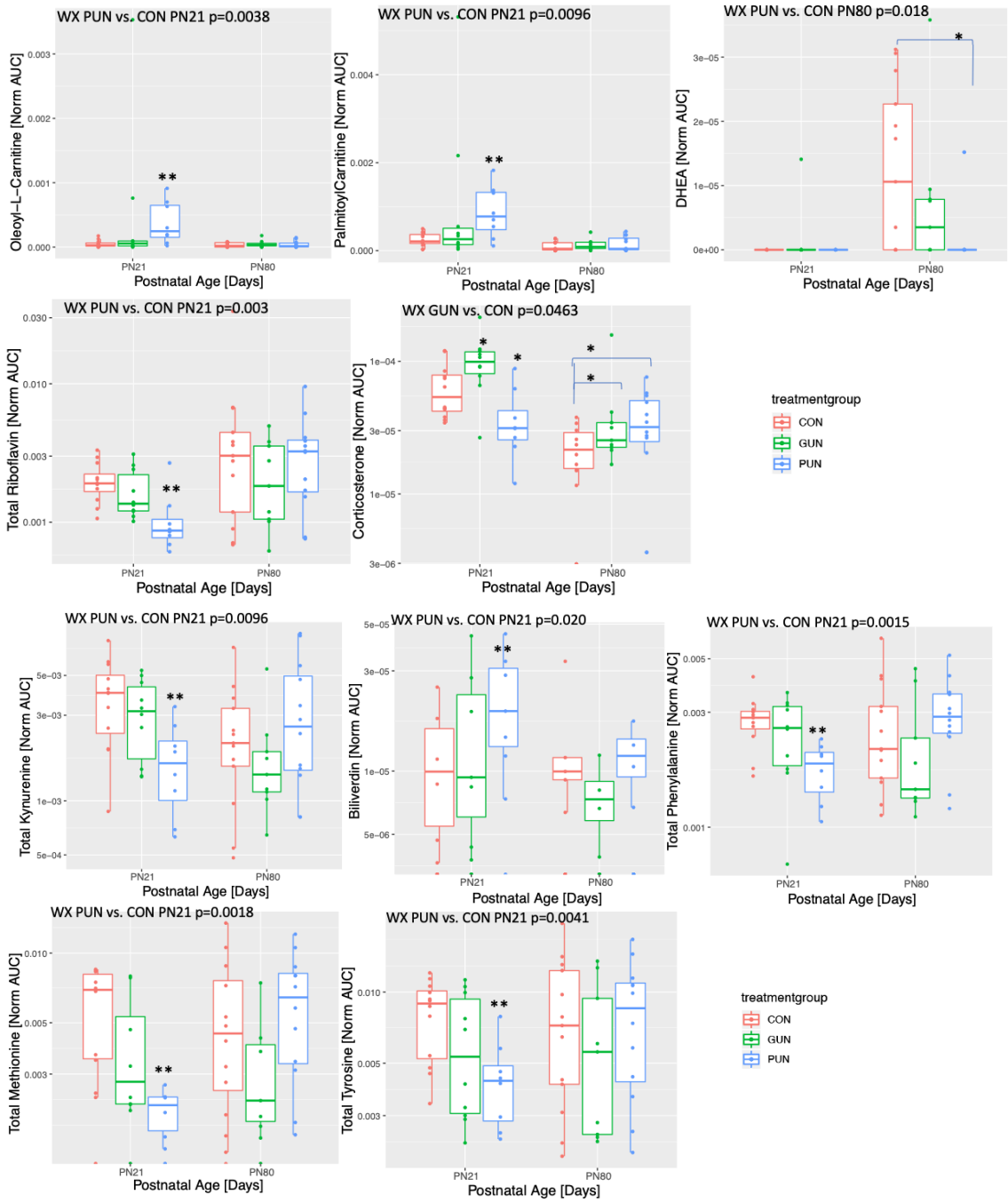

Figure 14: Liver Metabolites Between Treatment Groups at PN21 and PN80. Liver metabolite abundance was analyzed using a LMM in control (CON), gestationally undernourished (GUN), and postnatally undernourished (PUN) mice during young adolescent (PN21; CON n=12; GUN n=10; PUN n=8) and adulthood (PN80; CON n=12; GUN n=9; PUN n=12). PUN had abnormally low abundance compared to CON at PN21 in Cholic Acid (p=0.001), Muricholic Acid (p<0.001), Glycocholic Acid (p=0.03), Taurocholic Acid (p=0.0079), Total Bile Acids (sum of primary and secondary; p=0.0064), Riboflavin (p=0.003), and Total EAAs: Methionine (p=0.0018), Phenylalanine (p=0.0015), and Tyrosine (p=0.0041). In contrast, PUN had abnormally high levels of Oleoyl L-Carnitine (p=0.0038) and Palmitoyl carnitine (p=0.0096) and Biliverdin (p=0.020), but these recovered at PN80. Corticosterone was significantly overexpressed in GUN compared to PUN and CON at PN21 (p=0.043) and did not recover

at PN80. DHEA was the only metabolite to remain significantly low in PUN at PN80 compared to GUN and CON (p=0.018). The box portion of the boxplots represents the mean and interquartile ranges, lines on the boxplots are the standard deviations, and the dots represent the actual data points in the data set (WX=Wilcoxon Pairwise Comparison; p-value notation: *<0.05, **<0.01, ***<0.0001.)

Figure 14 (cont'd)

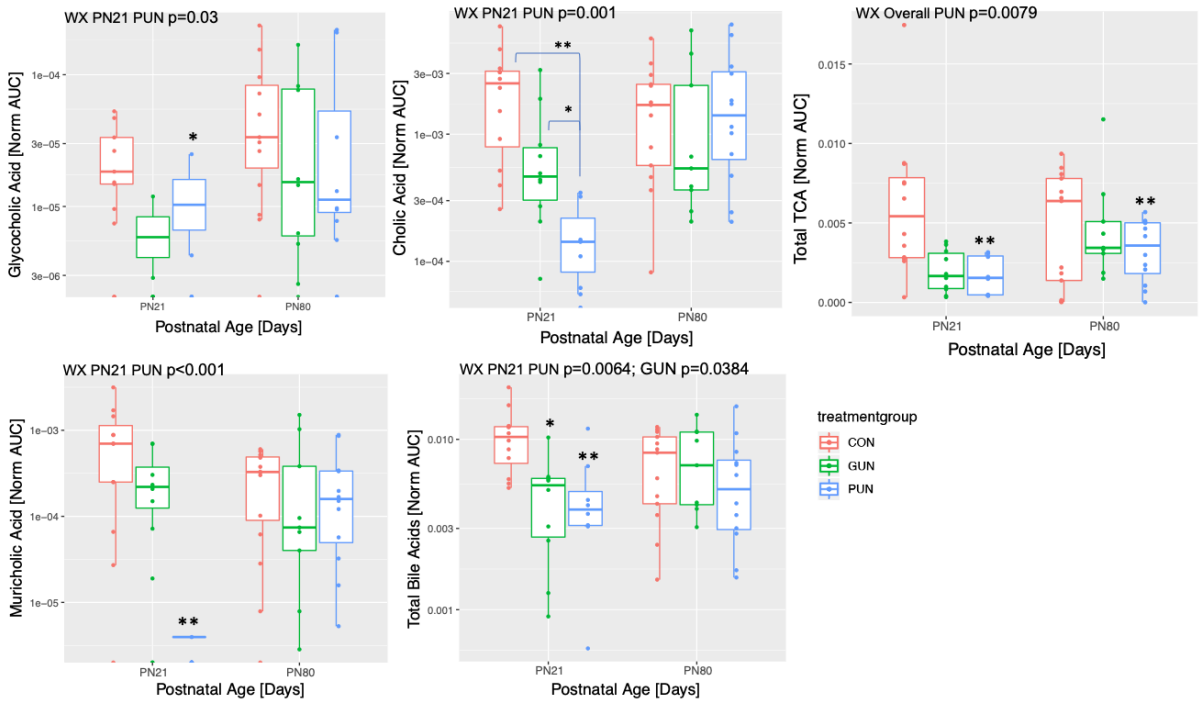

Fecal Metabolomics

The RF analysis of the fecal metabolome showed strong overall classification by treatment group (OOB error = 15.4%). The VIP of the RF classification showed that the strongest classifiers above a MDA of 5.0 were unknown molecules except for small peptides. Thus, the peptides were analyzed individually and collectively through time (weeks 1-5). Individual peptides were found with varied trends between the treatment groups, however most resulted in higher levels in GUN and PUN compared to CON. In light of this, all known peptides in the dataset were summed and compared to their overall abundances through the experiment. Total summed peptides were significantly higher in PUN compared

to CON (LMM p=0.0064; Tukey's: p=0.017), with slopes of m=-7 e^{-05} for PUN, m=-0.0003 for GUN and m=0.0016 for CON (Fig.15). ANCOVA slope comparison analysis revealed Serine-Valine (Ser-Val) was significantly higher in PUN (p=0.001) and GUN (p<0.0001) compared to CON. Serine-Isoleucine-Serine (Ser-Ile-Ser) was significantly higher in PUN (p=0.0008) compared to GUN and CON. Asparagine-Valine (Asn-Val; p<0.0001) and Glutamine-Methionine (Gln-Met; p=0.0029) were significantly higher in GUN compared to CON.

After the peptide analysis, LMM were performed on other metabolites in the VIP, revealing significant differences in various carnitines, reflecting altered end-products of lipid metabolism. (Table 3; Fig. 14) At PN21, PUN had significantly higher Hydroxybutyrylcarnitine (p≤0.0001) compared to CON

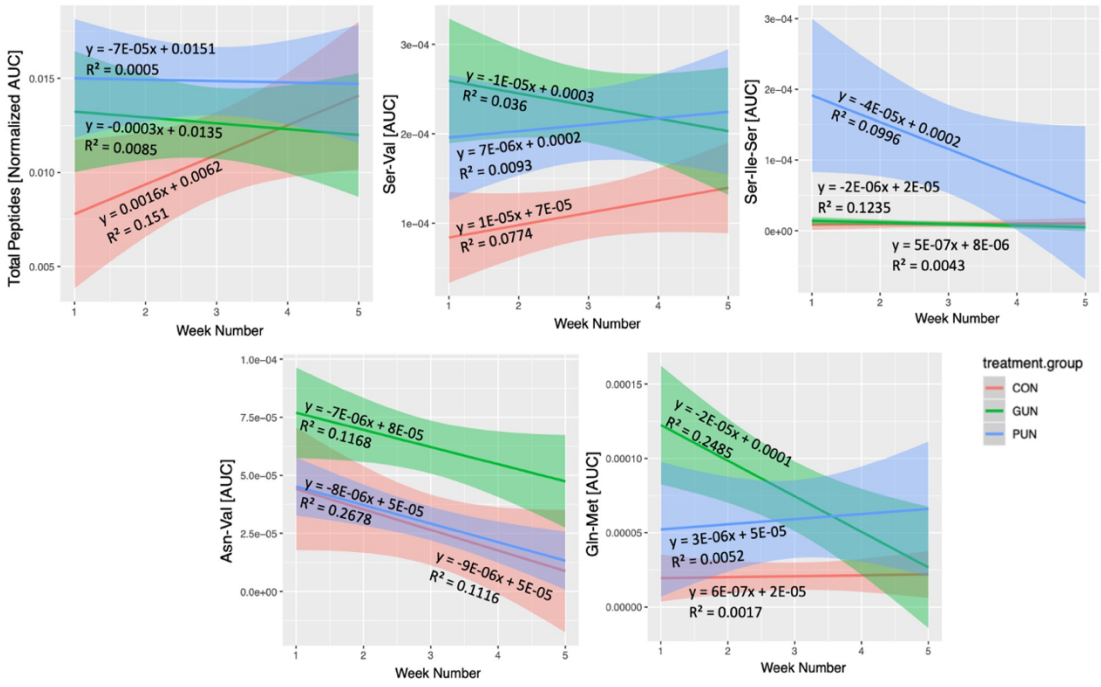

Figure 15: Fecal Peptide Linear Regression Analysis of GUN, PUN and CON from Week 1 through 5. Fecal peptides measured from fecal samples taken once per week for 5 weeks in CON (n=9), GUN (n=12), and PUN (n=11) mice analyzed via linear regression revealed an overall higher abundance of total peptides in PUN (overall: LMM p=0.0064) compared to CON across the lifespan (top-left). ANCOVA analysis revealed Serine-Valine (Ser-Val) was significantly higher in PUN (p=0.001) and GUN (p<0.0001) compared to CON. Serine-Isoleucine-Serine (Ser-Ile-Ser) was significantly higher in PUN (p=0.0008) compared to GUN and CON. Asparagine-Valine (Asn-Val; p<0.0001) and Glutamine-Methionine (Gln-Met; p=0.0029) were significantly higher in GUN compared to CON. The covariate used in this analysis was time (week number).

and higher Arachidonylcarnitine (p≤0.0001) compared to GUN. GUN also had significantly higher Hydroxybutyrylcarnitine p=0.0095) compared to CON over the 5-week duration. Alternatively, GUN had significantly lower hydroxyhexadecanoylcarnitine (p=0.0005) compared to CON over weeks 1-5 (Fig. 16).

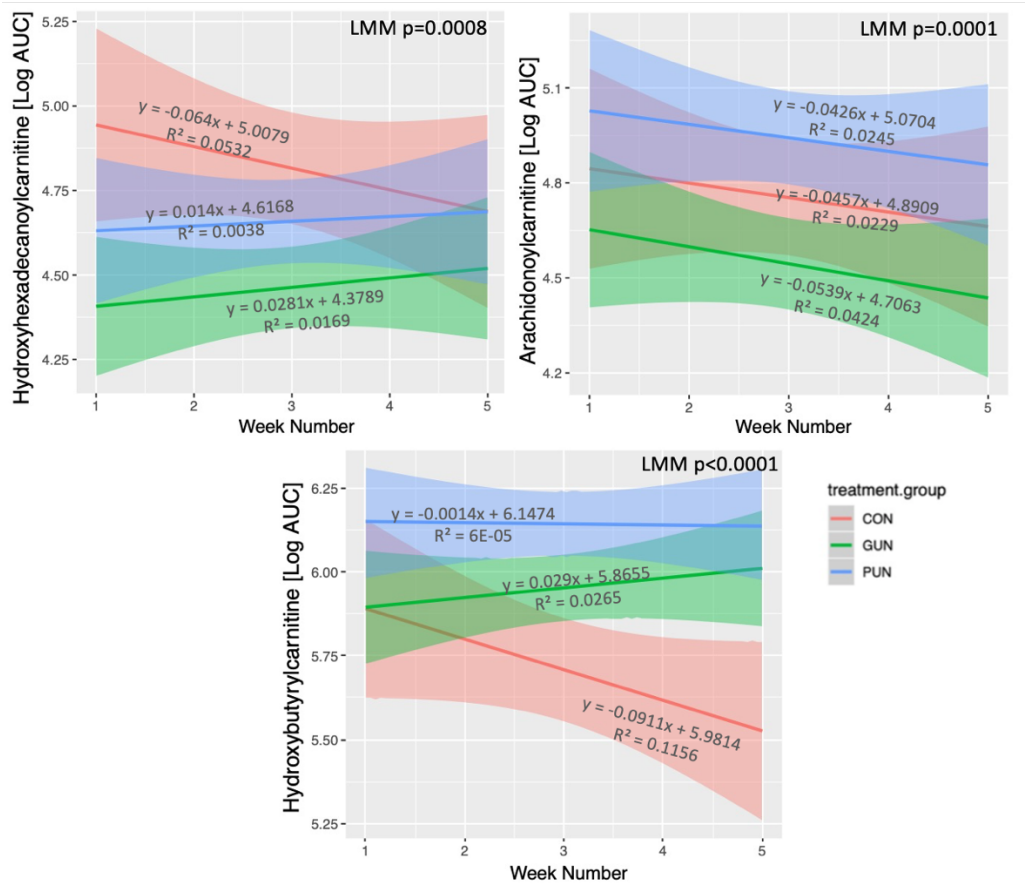

Figure 16: Fecal Metabolites Between Treatment Groups from Weeks 1 through 5. Linear regression and LMM Analysis resulted in PUN having overall higher Hydroxybutyrylcarnitine (p≤0.0001) and compared to CON and higher Arachidonylcarnitine (p≤0.0001) compared to GUN. GUN also had significantly higher Hydroxybutyrylcarnitine compared to CON (p=0.0095) and alternatively, significantly lower Hydroxyhexadecanoylcarnitine (p=0.0005) compared to CON over the 5-week duration.

Table 4: Fecal Metabolites between PUN, GUN, and CON at PN21 and PN80.

Metabolite	*Recovered(Y/N)*	*Physiological Relevance*
Hydroxybutyrlcarnitine	Y	Ketocarnitine; During fasting causes metabolic switch from glucose to fatty acid ß-oxidation for energy production
Arachidonylcarnitine	Y	Acylcarnitine; Abnormally high levels can indicate onset of insulin resistance
Hydroxyhexadecanoylcarnitine	Y	Acylcarnitine; Transports long-chain fatty acids into the matrix of the mitochondrion for β-oxidation

LMM analysis of fecal metabolites revealed most significant differences were in PUN and GUN compared to CON in various acylcarnitines, reflecting altered metabolic end-products of lipid metabolism. All fecal carnitines recovered to levels similar to CON by adulthood (PN80).

Cecum Metabolomics

The cecum metabolomes were first analyzed via RF resulting in an OOB error rate of 100% for PN21 and 93% for PN80, indicating very poor level of classification into respective treatment groups and an abnormally high rate of false discovery. Thus, no further metabolomic analysis was performed on the cecum samples.

DISCUSSION

The objective of the present study was to characterize the effects of undernutrition-induced growth restriction during two separate windows of development: gestation and postnatal life. Additionally, a primary focus was to highlight strong alterations in the metabolome, thus elucidating potential future directions in creating therapeutic measures to alleviate or prevent disease onset in adulthood and influence full growth and development in the undernourished population.

The overarching hypothesis of this study was that early life growth-restriction causes gut dysbiosis and an altered metabolome characterized by decreased B-Vitamin bioavailability, leading to impaired hepatic and muscle IGF-1 expression and growth restriction across the lifespan. The majority of the overarching hypothesis has been validated in the present study, as the microbiome and metabolome were both disrupted, IGF-1 expression was reduced and vitamin B_2 was lower in the growth restricted PUN group. However, not all B-vitamins were detected in the untargeted metabolomics data, somewhat limiting the B-vitamin bioavailability hypothesis. Despite this limitation, the untargeted metabolomics approach allowed for detection of thousands of other molecules that had not be previously measured. For example, there was a lower DHEA in adulthood, significant reductions in EAAs (i.e. Methionine) and disruptions in bile acid and carnitine metabolism. All of this corresponded to decreased IGF-1 expression in the liver and muscle of the PUN group.

Examining Longitudinal Microbial Differences between Treatment Groups

One of the main focuses of the present study was to determine the longitudinal microbial differences between growth restriction induced during gestation and during lactation. Fecal samples were collected weekly from PN18-PN80. Microbial structure and diversity were compared between diet groups over

time. We hypothesized that GUN and PUN mice will have microbiome dysbiosis compared to CON across the lifespan and the dysbiosis will be represented by decreased *Bifidobacterium* and *Lactobacilli*. The present study characterized the effects of growth restriction on the gut microbiome, with the largest differences seen in undernourishment during the postnatal window. Alpha-Diversity, or microbial complexity, remained significantly higher in PUN compared to CON into adulthood and increased slightly over time which is expected during gut microbiome development[55,144,145]. While diversity is generally considered a benefit to gut health[146], having a greater number of species in early life could be detrimental to the specific role the microbiome plays during development. It is possible that increased presence of unfavorable, unknown species and potential lack of some vital microbes from CON mice may contribute to the health disparities that manifests later in life in the PUN group. Additionally, GUN initially had a similar level of diversity to PUN, but recovered in adulthood, indicating the maturity or imprinting of the gut microbiome occurs during a key window of development (PN1-21) also found in various studies using this mouse model[6,7,88].

In order to determine specific microbial differences between the treatment groups beta diversity and phylogenetic analysis was performed. Phylogenetic analysis lead to the confirmation that a stunting effect occurred in the microbiome in PUN mice, which was exhibited by the majority of microbes present throughout the lifespan were reflective of those found mostly in infants. The *Bacteroides* and *Bifidobacterium* genera were higher in the PUN microbiome compared to GUN and CON and are well known for their complex and simple sugar fermentations for their own energy and growth needs[147–150]. Thus, initial abundance of these organisms in PUN in early life may be due to the mother's milk composition having a lower relative protein concentration and higher relative concentration of carbohydrates[151]. However, as seen in healthy normal guts, *Bifidobacterium* is highest in abundance at birth and during the breastfeeding stages and then begins to decrease in abundance into adulthood where it then maintains in much lower levels[152]. While these microbes may have potential benefits in early life,

their presence at abnormally high levels in adulthood could lead to a multitude of detrimental effects due to their production of unfavorable short-chain fatty acids (SCFAs)[153–156].

Many studies have shown that *Bifidobacterium* and *Bacteroides* make other byproducts in addition to SCFAs that in much higher quantity, actually degrade specific gut physiology that aid in regulating nutrient absorption and can progress to severe malnutrition and disease development. Belenguer et al. 2007, showed that when *Bifidobacterium* colonization increases beyond normal levels, fermentative byproducts acetate and lactate increase, decreasing the amount of available butyrate[154]. Additionally, high abundance of *Bacteroides* is also linked to decreased butyrate concentrations[157] which can induce degradation of the gut's mucin layer and compromise the condition of the tight junctions between epithelial cells involved in nutrient absorption and immune protection[157].

Potential evidence of altered nutrient absorption in PUN mice was exhibited by abnormally high levels of excreted peptides in the fecal samples. Additionally, high levels of excreted peptides in the PUN mice lasted throughout the lifespan despite refeeding of the CON diet, indicating there is potential programming occurring in the intestinal tract. Generally, larger amino acids are broken down in the stomach and smaller di- and tripeptides are absorbed into the small intestine epithelium via peptide transporters (PepT1)[158]. PepT1 transports peptides into the enterocyte, and then cytoplasmic peptidases break them down into amino acids and export them out of the cell and into the bloodstream[158]. Since the di- and tripeptides are found in the fecal samples, this signifies an inability to absorb/transport them from the lumen into the enterocytes. It is possible that this transport capability in PUN mice may be altered during early life programming. Further research is necessary to determine the effects of postnatal growth restriction on PepT1.

Examining Effects of Growth Restriction on the Liver and Fecal Metabolome

The primary focus of Aim 2 was to determine the effects of growth restriction on the metabolome in GUN, PUN and CON mice. Cecum and livers were collected at two timepoints: PN21 and PN80 and fecal samples were collected through the lifespan. Cecums were collected due to their function as a reservoir of metabolites produced from the mouse as well as their intestinal microbes. We hypothesized that growth restriction would negatively alter the metabolome in PUN and GUN mice with B-Vitamins, such as folate and B-12, primarily shaping the differences. Unfortunately, due to the untargeted nature of the metabolomics methods used, we did not detect all B-vitamins. Folate and B-12 were not found in the sample set, either due inefficient extraction of the compounds in the methanol solvent or them being below the detection limit. Riboflavin (B_2), however, was found to be significantly reduced in PUN livers at PN21, as hypothesized. B_2 deficiencies can also lead to various developmental abnormalities including growth restriction and cardiovascular disease[159]. Without adequate amounts of B_2, carbohydrates, fat and protein are not able to be digested appropriately, leading to disparities in energy balance and potentially elucidating the abnormally high excretion of fecal peptides in PUN mice found in this study[160].

Other impairments in the PUN mice were in protein synthesis/growth-regulating metabolites: methionine, phenylalanine, tyrosine and DHEA as well as metabolism-regulating metabolites: decreased primary bile acids and increased acylcarnitines.

Protein-Synthesis and Growth-Regulating Metabolites

This study confirmed that growth restriction during postnatal life leads to decreased methionine which is vital in the synthesis of all subsequent proteins in addition to DNA and cellular methylation[161,162]. There was a significant reduction in methionine, phenylalanine, tyrosine and a trending lower expression of tryptophan, which are all vital to the absorption, utilization and synthesis of subsequent proteins[163]. Methionine is a sulfur-containing EAA that is not produced endogenously and must be received in the diet. Methionine is a precursor to a variety of other vital components of

metabolism such as succinyl-coA, homocysteine, cysteine and carnitine[161]. Methionine is also a precursor to cellular methylation and may have an essential role in gene regulation due to its upstream role in cell proliferation[130,162,164]. B_2 is a cofactor for methionine activation[164] which may elucidate why both were significantly low in PUN at PN21. B_2 and methionine are both vital to regulating sulfur and one-carbon metabolism in gut microbes for survival[164–166]. Since both B_2 and methionine were significantly low, this increases the possibility of a competition for resources between the gut microbes and the host, altering the bacterial species that are able to survive and leaving the host with B_2 and subsequently methionine and B_3 (niacin) deficiencies further increasing risk of disease onset[167,168].

Methionine & Cellular Stress

Methionine also has an important role in regulating reactive oxygen species (ROS) production and glutathione biosynthesis which mainly act as antioxidants and help to prevent oxidative damage in tissues like the liver and heart mitochondria[161]. Mitochondria are organelles within cells that are essential for cell proliferation and survival[169]. They produce energy to fuel countless processes (adenosine triphosphate; ATP), control intracellular calcium (Ca^{2+}) and cell differentiation[169]. In the present study, glutathione was not significantly different among treatment groups however it trended lower in PUN mice at PN21. Many studies have shown correlations between early life growth restriction and impaired mitochondrial function[170,171]. Gomez et al. in 2015 showed that methionine can potentially reverse the effects of oxidative damage involving complex I of the electron transport chain[172]. Additionally, cysteine, which is another sulfur-containing amino acid, showed improvement in reversing mitochondrial oxidative damage in complex I[172]. Cystathionine, a precursor to cysteine, trended very low in PUN mice at PN21, suggesting that both sources for sulfur-containing amino acids are stunted in the growth restricted mice and the capacity to overcome oxidative stress and cellular damage is also impaired.

Metabolism-Regulating Metabolites: Liver Bile Acids and AcylCarnitines

One of the more unexpected findings in this study was the substantial decrease in primary bile acid production and increases in liver acylcarnitines, both of which recovered in adulthood. These alterations may be a direct result of the diet differences between the treatment groups but may too have an imprint on disease pathways related to fat metabolism in the liver into adulthood[173–175]. Moreover, there is a potential connection between bile acid synthesis and reduced methionine at PN21 in PUN mice. A study by Hasek et al. 2013 showed that methionine restriction, via gene regulation, decreases liver triglyceride synthesis, deposition, exportation and increases beta oxidation and fat utilization[176]. Since bile acids are made from cholesterol[177–179], when liver triglycerides are reduced, there will be a subsequent reduction in bile acid synthesis. PUN mice had a significant reduction in all primary bile acids: taurocholic acid (TCA), glycocholic acid (GCA), cholic acid (CA) and muricholic acid (MCA) at PN21. At PN80, the bile acid abundances normalized, indicating their abundance is influenced primarily by suckling from low protein fed dams and not indicative of permanent metabolic reprogramming.

Determining Longitudinal Effects of Growth Restriction on Growth Parameters & Regulators

In order to determine the longitudinal effects of growth-restriction on IGF-1 expression in liver and muscle (GS) in Aim 3, western blots were completed comparing diet groups (CON, GUN, and PUN) at PN21 and PN80. The overall hypothesis for Aim 3 was that there would be decreased levels of IGF-1 in the PUN and GUN mice, resulting in decreased overall body weight and muscle mass. The present study confirmed that growth restriction during the postnatal window leads to a significant reduction in growth markers including overall bodyweight, muscle mass, hepatic Dehydroepiandrosterone (DHEA) and muscular IGF-1 expression. Hepatic IGF-1 expression at was significantly lower at PN21 in GUN and PUN mice compared to control, and GS was also overall lower over time.

DHEA & IGF-1 Expression

A study by Bieswal et al. 2006, showed that protein- or calorie-restriction during postnatal development of life leads to permanent longitudinal growth stunting and reduced body weight[23]. The findings by Bieswal et al. correlate well with this study since GUN did experience catch-up growth but PUN did not despite refeeding. Refeeding involved increasing protein by ~12% at PN21 (4% more than in Bieswal's study) and levels of EAAs recovered, the postnatal programming effects permanently reduced body weights and muscle mass into adulthood compared to CON. Additionally, after refeeding for approximately 59 days, there was an extremely low abundance of DHEA in PUN at PN80, signifying another trend of permanent programming lasting into adulthood. DHEA is an endogenous adrenal androgen synthesized from cholesterol and is a precursor to estrogen and testosterone. DHEA increases muscle hypertrophy[180], IGF-1 bioavailability[181] and has protective effects against insulin resistance[182] cardiovascular disease[183], and cancer[184].

A study by Fiorotto et al. 2014, established that postnatally-restricted mice had low expression of mammalian target of rapamycin (mTOR) and phosphorylated mTOR[22]. The present study confirmed that IGF-1 was significantly decreased in the liver at PN21 and overall lower in muscle in PUN and GUN compared to CON, which correlates well to the reflecting low expression of liver DHEA in adulthood. DHEA increases IGF-1 bioavailability, facilitating activation of the mTOR pathway[181,185]. Thus, not only was the ability to grow initially stunted via a significant reduction in growth-dependent amino acids (i.e. Methionine, Phenylalanine, Tyrosine, Tryptophan) and IGF-1 expression, but also continually reduced via an inability to produce DHEA in adulthood.

Limitations and Future Directions

A main caveat to this study is that the LC-MS/MS metabolomics approach used is an untargeted exploratory method which primarily identifies more non-polar, larger molecules. Thousands of molecules are profiled in a single experiment, which greatly aids in power for discovery, however since the method

is untargeted LC-MS/MS, certain compounds like SCFAs and certain B-Vitamins are impossible to find in the sample set. Gas chromatography-mass spectrometry (GC/MS-MS) is better suited for analysis of SCFAs that are known to be produced by *Bacteroides* spp. and targeted measurements of each B-Vitamin will be required to assay this metabolite group. Additionally, future studies should look deeper into the mechanistic impact SCFAs have in the undernourished and growth restricted populations. Future studies should also measure FXR and TGR5 to determine if undernutrition and alteration of the gut microbiome via growth restriction reduces their expression and/or signaling activity via either GLP-1 or the mTOR pathway. Lastly, a final caveat of this project is to ensure larger sample sizes are generated for each sex and diet group regardless of examining sex effects in order to account for natural occurrences that may lead to eliminating mice from the study in future research and to lower variability that may occur in uneven sex samples. Although there was no preliminary data showing effect size with growth restriction and the microbiome and metabolome, hopefully this data can act as a baseline or preliminary basis to build upon in forthcoming research.

CONCLUSION

The present study showed that the gut microbiome and metabolome are significantly altered by early-life growth restriction, particularly in those mice that are undernourished during the PN1-21 developmental window. The microbiome dysbiosis observed was likely primarily due to an elevated abundance of *Bacteroides* spp., a group of sugar fermenters common in the mammalian gut. There may be mechanisms to manipulate the microbiome by reducing the abundance of *Bacteroides* spp. through probiotic or prebiotic means, to help reduce the effects of undernutrition, but future work is needed to understand how this bacterial group contributes to the disease manifestations seen in adulthood.

Metabolites in the liver, such as the significant deficits in methionine and an increase in excretion of peptides strongly signifying detrimental metabolic alterations that could contribute to the onset of various disease states. Additionally, the metabolic mechanism significantly reducing DHEA abundance in PUN may be a crucial area to continue to explore as this metabolite has various roles in early life growth and development in addition to regulation of hormones and normal physiological processes in adulthood.

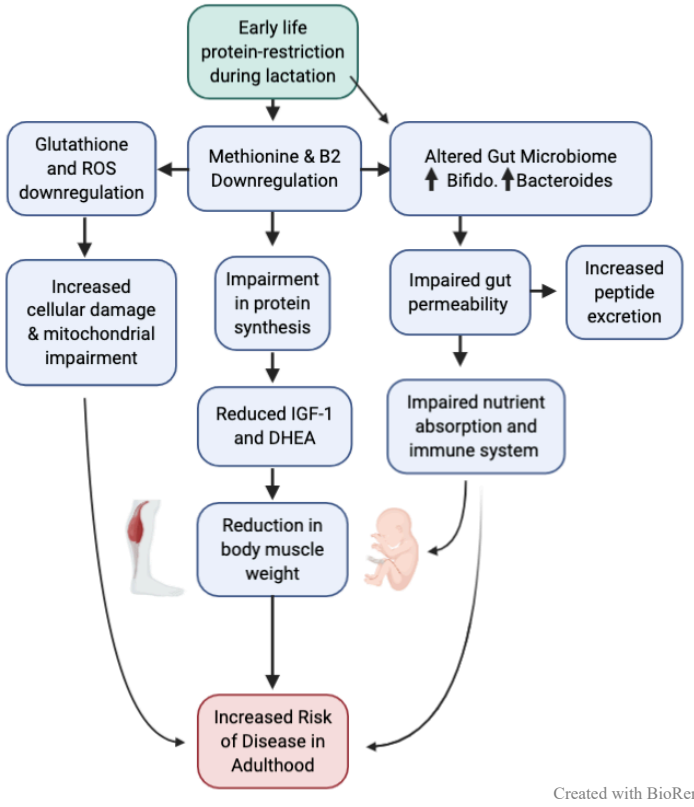

Figure 17: Proposed Effects of Global Caloric Restriction During Postnatal Development

The overarching hypothesis of this study was that gestational and postnatal growth-restriction leads to gut dysbiosis, decreased B-Vitamin bioavailability, impaired hepatic and muscle IGF-1 expression and across the lifespan. Metabolic impairments resulting from growth restriction are evident by an altered gut microbiome which leads to impaired gut permeability, impaired nutrient absorption and increased peptide excretion. Postnatal growth restriction is caused by downregulation of methionine, B_2, IGF-1 and DHEA which are necessary for proper growth and development. Other potential correlations include methionine reduction and an associated impairment in controlling oxidative stress (or Reactive Oxygen Species; ROS) and cellular damage in the mitochondria.

REFERENCES

1. Lawn, J. E. *et al.* Every newborn: Progress, priorities, and potential beyond survival. *The Lancet* vol. 384 189–205 (2014).

2. Morrison, J. L. *et al.* Restriction of placental function alters heart development in the sheep fetus. *Am. J. Physiol. Integr. Comp. Physiol.* (2007) doi:10.1152/ajpregu.00798.2006.

3. Fernandez-Twinn, D. S. *et al.* The maternal endocrine environment in the low-protein model of intra-uterine growth restriction. *Br. J. Nutr.* **90**, 815–822 (2003).

4. Barker, D. J. In utero programming of chronic disease. *Clin. Sci. (Lond).* (1998).

5. Barker, D. J. P. The origins of the developmental origins theory. in *Journal of Internal Medicine* (2007). doi:10.1111/j.1365-2796.2007.01809.x.

6. Leszczynski, E. C., Visker, J. R. & Ferguson, D. P. The Effect of Growth Restriction on Voluntary Physical Activity Engagement in Mice. *Med. Sci. Sport. Exerc.* 1 (2019) doi:10.1249/MSS.0000000000002040.

7. Visker, J. R. & Ferguson, D. P. Postnatal undernutrition in mice causes cardiac arrhythmogenesis which is exacerbated when pharmacologically stressed. *J. Dev. Orig. Health Dis.* **9**, 417–424 (2018).

8. Mentch, S. J. & Locasale, J. W. One-carbon metabolism and epigenetics: understanding the specificity. *Ann. N. Y. Acad. Sci.* **1363**, 91–8 (2016).

9. Crider, K. S., Yang, T. P., Berry, R. J. & Bailey, L. B. Folate and DNA Methylation: A Review of Molecular Mechanisms and the Evidence for Folate's Role. *Adv. Nutr.* **3**, 21–38 (2012).

10. Rosario, F. J., Nathanielsz, P. W., Powell, T. L. & Jansson, T. Maternal folate deficiency causes inhibition of mTOR signaling, down-regulation of placental amino acid transporters and fetal growth restriction in mice. *Sci. Rep.* **7**, 3982 (2017).

11. Roman-Garcia, P. *et al.* Vitamin B12–dependent taurine synthesis regulates growth and bone

mass. *J. Clin. Invest.* **124**, 2988–3002 (2014).

12. Vernocchi, P., Del Chierico, F. & Putignani, L. Gut Microbiota Profiling: Metabolomics Based Approach to Unravel Compounds Affecting Human Health. *Front. Microbiol.* **7**, 1144 (2016).

13. Schwarzer, M. *et al.* Lactobacillus plantarum strain maintains growth of infant mice during chronic undernutrition . *Science (80-.).* **351**, 854–857 (2016).

14. Roseboom, T., de Rooij, S. & Painter, R. The Dutch famine and its long-term consequences for adult health. *Early Human Development* (2006) doi:10.1016/j.earlhumdev.2006.07.001.

15. Painter, R. C., Roseboom, T. J. & Bleker, O. P. Prenatal exposure to the Dutch famine and disease in later life: An overview. *Reproductive Toxicology* vol. 20 345–352 (2005).

16. Dalvi, P. S. *et al.* Long-term metabolic effects of malnutrition: Liver steatosis and insulin resistance following early-life protein restriction. *PLoS One* **13**, e0199916 (2018).

17. Barker, D. J. P., Osmond, C., Kajantie, E. & Eriksson, J. G. Growth and chronic disease: Findings in the Helsinki Birth Cohort. *Ann. Hum. Biol.* **36**, 444–458 (2009).

18. Sandboge, S. *et al.* Early growth and non-alcoholic fatty liver disease in adulthood—the NAFLD liver fat score and equation applied on the Helsinki Birth Cohort Study. *Ann. Med.* **45**, 430–437 (2013).

19. Nguyen, T. L. A., Vieira-Silva, S., Liston, A. & Raes, J. How informative is the mouse for human gut microbiota research? *Dis. Model. Mech.* **8**, 1–16 (2015).

20. Ferguson, D. P. *et al.* Postnatal undernutrition alters adult female mouse cardiac structure and function leading to limited exercise capacity. *J. Physiol.* (2019) doi:10.1113/JP277637.

21. Schmidt, M. *et al.* Influence of low protein diet-induced fetal growth restriction on the neuroplacental corticosterone axis in the rat. *Front. Endocrinol. (Lausanne).* **10**, (2019).

22. Fiorotto, M. L. *et al.* Ribosome abundance regulates the recovery of skeletal muscle protein mass upon recuperation from postnatal undernutrition in mice. *J. Physiol.* (2014) doi:10.1113/jphysiol.2014.279067.

23. Bieswal, F. *et al.* The importance of catch-up growth after early malnutrition for the programming of obesity in male rat. *Obesity* (2006) doi:10.1038/oby.2006.151.

24. Ketelslegers, J. M., Maiter, D., Maes, M., Underwood, L. E. & Thissen, J. P. Nutritional regulation of insulin-like growth factor-I. *Metabolism* (1995) doi:10.1016/0026-0495(95)90221-X.

25. Watkins, A. J. *et al.* Low protein diet fed exclusively during mouse oocyte maturation leads to behavioural and cardiovascular abnormalities in offspring. *J. Physiol.* (2008) doi:10.1113/jphysiol.2007.149229.

26. Schwarzer, M. *et al.* Lactobacillus plantarum strain maintains growth of infant mice during chronic undernutrition. *Science (80-.).* **351**, 854–857 (2016).

27. Blondeau, B., Lesage, J., Czernichow, P., Dupouy, J. P. & Bréant, B. Glucocorticoids impair fetal β-cell development in rats. *Am. J. Physiol. - Endocrinol. Metab.* (2001) doi:10.1152/ajpendo.2001.281.3.e592.

28. Isganaitis, E. *et al.* Accelerated postnatal growth increases lipogenic gene expression and adipocyte size in low-birth weight mice. *Diabetes* (2009) doi:10.2337/db08-1266.

29. Ma, H. *et al.* Attenuated Effects of Bile Acids on Glucose Metabolism and Insulin Sensitivity in a Male Mouse Model of Prenatal Undernutrition. *Endocrinology* **158**, 2441–2452 (2017).

30. Wattez, J. S. *et al.* Maternal perinatal undernutrition modifies lactose and serotranferrin in milk: Relevance to the programming of metabolic diseases? *Am. J. Physiol. - Endocrinol. Metab.* (2015) doi:10.1152/ajpendo.00452.2014.

31. Wolfe, D. *et al.* Nutrient sensor–mediated programmed nonalcoholic fatty liver disease in low birthweight offspring. *Am. J. Obstet. Gynecol.* **207**, 308.e1-308.e6 (2012).

32. Preidis, G. A. *et al.* Microbial-Derived Metabolites Reflect an Altered Intestinal Microbiota during Catch-Up Growth in Undernourished Neonatal Mice. *J. Nutr.* **146**, 940–948 (2016).

33. Preidis, G. A. *et al.* Composition and function of the undernourished neonatal mouse intestinal microbiome. *J. Nutr. Biochem.* **26**, 1050–1057 (2015).

34. Preidis, G. A. *et al.* The Undernourished Neonatal Mouse Metabolome Reveals Evidence of Liver and Biliary Dysfunction, Inflammation, and Oxidative Stress 1-3. *Proteomics, Metabolomics J. Nutr* **144**, 273–281 (2014).

35. Martínez, D. *et al.* In Utero Undernutrition in Male Mice Programs Liver Lipid Metabolism in the Second-Generation Offspring Involving Altered Lxra DNA Methylation. *Cell Metab.* **19**, 941–951 (2014).

36. Beauchamp, B. *et al.* Undernutrition during pregnancy in mice leads to dysfunctional cardiac muscle respiration in adult offspring. *Biosci. Rep.* **35**, (2015).

37. Dwyer, C. M. & Stickland, N. C. The effects of maternal undernutrition on maternal and fetal serum insulin-like growth factors, thyroid hormones and cortisol in the guinea pig. *J. Dev. Physiol.* (1992).

38. Treuting, P. M. & Dintzis, S. M. *Comparative Anatomy and Histology: A Mouse and Human Atlas 12. Lower Gastrointestinal Tract*. *Comparative Anatomy and Histology* (2012).

39. Hugenholtz, F. & de Vos, W. M. Mouse models for human intestinal microbiota research: a critical evaluation. *Cellular and Molecular Life Sciences* vol. 75 149–160 (2018).

40. Justice, M. J. & Dhillon, P. Using the mouse to model human disease: increasing validity and reproducibility. *Dis. Model. Mech.* **9**, 101–3 (2016).

41. Wos-Oxley, M. L. *et al.* Comparative evaluation of establishing a human gut microbial community within rodent models. *Gut Microbes* **3**, 1–16 (2012).

42. Uhlig, H. H. & Powrie, F. Mouse models of intestinal inflammation as tools to understand the pathogenesis of inflammatory bowel disease. *European Journal of Immunology* (2009) doi:10.1002/eji.200939602.

43. Wirtz, S. & Neurath, M. F. Mouse models of inflammatory bowel disease. *Advanced Drug Delivery Reviews* (2007) doi:10.1016/j.addr.2007.07.003.

44. Pizarro, T. T., Arseneau, K. O., Bamias, G. & Cominelli, F. Mouse models for the study of Crohn's disease. *Trends in Molecular Medicine* (2003) doi:10.1016/S1471-4914(03)00052-2.

45. Gu, S. *et al.* Bacterial Community Mapping of the Mouse Gastrointestinal Tract. *PLoS One* (2013) doi:10.1371/journal.pone.0074957.

46. Wolin, M. J. Fermentation in the rumen and human large intestine. *Science (80-.).* (1981) doi:10.1126/science.7280665.

47. Marteau, P. *et al.* Comparative Study of Bacterial Groups within the Human Cecal and Fecal Microbiota. *Appl. Environ. Microbiol.* (2001) doi:10.1128/AEM.67.10.4939-4942.2001.

48. Smith, H. F. *et al.* Comparative anatomy and phylogenetic distribution of the mammalian cecal appendix. *J. Evol. Biol.* (2009) doi:10.1111/j.1420-9101.2009.01809.x.

49. Smith, H. F., Parker, W., Kotzé, S. H. & Laurin, M. Multiple independent appearances of the cecal appendix in mammalian evolution and an investigation of related ecological and anatomical factors. *Comptes Rendus - Palevol* (2013) doi:10.1016/j.crpv.2012.12.001.

50. Snipes, R. L. Anatomy of the cecum of the laboratory mouse and rat. *Anat. Embryol. (Berl).* (1981) doi:10.1007/BF00301871.

51. Rowland, I. *et al.* Gut microbiota functions: metabolism of nutrients and other food components. *Eur. J. Nutr.* **57**, 1–24 (2018).

52. Voreades, N., Kozil, A. & Weir, T. L. Diet and the development of the human intestinal microbiome. *Front. Microbiol.* (2014) doi:10.3389/fmicb.2014.00494.

53. Xiong, W., Giannone, R. J., Morowitz, M. J., Banfield, J. F. & Hettich, R. L. Development of an enhanced metaproteomic approach for deepening the microbiome characterization of the human infant gut. *J. Proteome Res.* (2015) doi:10.1021/pr500936p.

54. Stewart, C. J. *et al.* Temporal development of the gut microbiome in early childhood from the TEDDY study. *Nature* (2018) doi:10.1038/s41586-018-0617-x.

55. Nagpal, R. *et al.* Gut microbiome and aging: Physiological and mechanistic insights. *Nutr. Heal. aging* **4**, 267–285 (2018).

56. Levi Mortera, S. *et al.* Monitoring Perinatal Gut Microbiota in Mouse Models by Mass Spectrometry Approaches: Parental Genetic Background and Breastfeeding Effects. *Front. Microbiol.* **7**, 1523 (2016).

57. Koenig, J. E. *et al.* Succession of microbial consortia in the developing infant gut microbiome. *Proc. Natl. Acad. Sci.* **108**, 4578–4585 (2011).

58. Patole, S. K. *et al.* Effect of Bifidobacterium breve M-16V supplementation on faecal bifidobacteria in growth restricted very preterm infants – analysis from a randomised trial. *J. Matern. Neonatal Med.* (2016) doi:10.3109/14767058.2016.1147554.

59. Arboleya, S., Watkins, C., Stanton, C. & Ross, R. P. Gut bifidobacteria populations in human health and aging. *Frontiers in Microbiology* (2016) doi:10.3389/fmicb.2016.01204.

60. Téfit, M. A. T. & Leulier, F. Lactobacillus plantarum favors the early emergence of fit and fertile adult Drosophila upon chronic undernutrition. (2017) doi:10.1242/jeb.151522.

61. Dutta, S. & Sengupta, P. Men and mice: Relating their ages. *Life Sciences* vol. 152 244–248 (2016).

62. Canfora, E. E., Jocken, J. W. & Blaak, E. E. Short-chain fatty acids in control of body weight and insulin sensitivity. *Nat. Rev. Endocrinol.* **11**, 577–591 (2015).

63. Sanna, S. *et al.* Causal relationships among the gut microbiome, short-chain fatty acids and metabolic diseases. *Nat. Genet.* **51**, 600–605 (2019).

64. Paparo, L. *et al.* The Influence of Fiber on Gut Microbiota: Butyrate as Molecular Player Involved in the Beneficial Interplay Between Dietary Fiber and Cardiovascular Health. *Diet. Fiber Prev. Cardiovasc. Dis.* 61–71 (2017) doi:10.1016/B978-0-12-805130-6.00004-5.

65. Dutta, S. & Sengupta, P. Men and mice: Relating their ages. *Life Sci.* **152**, 244–248 (2016).

66. D'Inca, R., Gras-Le Guen, C., Che, L., Sangild, P. T. & Le Huërou-Luron, I. Intrauterine growth restriction delays feeding-induced gut adaptation in term newborn pigs. *Neonatology* (2011) doi:10.1159/000314919.

67. Scott, J. M. Folate and vitamin B 12 . *Proc. Nutr. Soc.* (1999) doi:10.1017/s0029665199000580.

68. Strand, T. A. *et al.* Vitamin B-12, folic acid, and growth in 6- to 30-month-old children: A randomized controlled trial. *Pediatrics* (2015) doi:10.1542/peds.2014-1848.

69. Chen, Y. Y., Gupta, M. B., Grattton, R., Powell, T. L. & Jansson, T. Down-regulation of placental folate transporters in intrauterine growth restriction. *J. Nutr. Biochem.* **59**, 136–141 (2018).

70. Huang, S. *et al.* Characteristics of the gut microbiota colonization, inflammatory profile, and plasma metabolome in intrauterine growth restricted piglets during the first 12 hours after birth. *J. Microbiol.* **57**, 748–758 (2019).

71. Corfield, A. P., Carroll, D., Myerscough, N. & Probert, C. S. Mucins in the gastrointestinal tract in health and disease. *Frontiers in bioscience : a journal and virtual library* (2001) doi:10.2741/a684.

72. MacKie, A. R., Round, A. N., Rigby, N. M. & MacIerzanka, A. The Role of the Mucus Barrier in Digestion. *Food Digestion* (2012) doi:10.1007/s13228-012-0021-1.

73. Kim, S. H. *et al.* Three-dimensional intestinal villi epithelium enhances protection of human intestinal cells from bacterial infection by inducing mucin expression. *Integr. Biol. (United Kingdom)* (2014) doi:10.1039/c4ib00157e.

74. Delzenne, N. M. *et al.* Contribution of the gut microbiota to the regulation of host metabolism and energy balance: a focus on the gut–liver axis. *Proc. Nutr. Soc.* **78**, 319–328 (2019).

75. Chiang, J. Y. L. & Ferrell, J. M. Bile Acid Metabolism in Liver Pathobiology. *Gene Expr.* **18**, 71–87 (2018).

76. Blanton, L. V., Barratt, M. J., Charbonneau, M. R., Ahmed, T. & Gordon, J. I. Childhood undernutrition, the gut microbiota, and microbiota-directed therapeutics. *Science (80-.).* **352**, 1533–1533 (2016).

77. Poinsot, P., Schwarzer, M., Peretti, N. & Leulier, F. 40 years of IGF1: The emerging connections between IGF1, the intestinal microbiome, lactobacillus strains and bone growth. *Journal of Molecular Endocrinology* vol. 61 T103–T113 (2018).

78. Bonkowski, M. S. *et al.* Disruption of growth hormone receptor prevents calorie restriction from improving insulin action and longevity. *PLoS One* (2009) doi:10.1371/journal.pone.0004567.

79. Poinsot, P., Schwarzer, M., Peretti, N. & Leulier, F. 40 years of IGF1: The emerging connections between IGF1, the intestinal microbiome, lactobacillus strains and bone growth. *Journal of Molecular Endocrinology* (2018) doi:10.1530/JME-17-0292.

80. Yan, J. *et al.* Gut microbiota induce IGF-1 and promote bone formation and growth. *Proc. Natl. Acad. Sci. U. S. A.* **113**, E7554–E7563 (2016).

81. Langley-Evans, S. C. *Developmental programming of health and disease*. https://www.ncbi.nlm.nih.gov/pmc/articles/PMC1885472/pdf/nihms-346.pdf.

82. Aguirre, G. A., Ita, J. R., Garza, R. G. & Castilla-Cortazar, I. Insulin-like growth factor-1 deficiency and metabolic syndrome. *J. Transl. Med.* (2016) doi:10.1186/s12967-015-0762-z.

83. Holt, R. I. G. Fetal programming of the growth hormone-insulin-like growth factor axis. *Trends in Endocrinology and Metabolism* (2002) doi:10.1016/S1043-2760(02)00697-5.

84. Fazeli, P. K. & Klibanski, A. Determinants of GH resistance in malnutrition. *Journal of Endocrinology* vol. 220 (2014).

85. Kyriakakou, M. *et al.* The role of IGF-1 and Ghrelin in the compensation of intrauterine growth restriction. *Reprod. Sci.* (2009) doi:10.1177/1933719109344629.

86. Baker, J., Liu, J. P., Robertson, E. J. & Efstratiadis, A. Role of insulin-like growth factors in embryonic and postnatal growth. *Cell* **75**, 73–82 (1993).

87. LeRoith, D. & Yakar, S. Mechanisms of disease: Metabolic effects of growth hormone and insulin-like growth factor 1. *Nature Clinical Practice Endocrinology and Metabolism* (2007) doi:10.1038/ncpendmet0427.

88. Pendergrast, L. A., Leszczynski, E. C., Visker, J. R., Triplett, A. N. & Ferguson, D. P. Early life undernutrition reduces maximum treadmill running capacity in adulthood in mice. *Appl. Physiol. Nutr. Metab.* (2019) doi:10.1139/apnm-2019-0023.

89. Rondó, P. H. C. *et al.* Maternal psychological stress and distress as predictors of low birth weight, prematurity and intrauterine growth retardation. *Eur. J. Clin. Nutr.* **57**, 266–272 (2003).

90. Figueiredo, Í. L. *et al.* Prolonged maternal separation induces undernutrition and systemic inflammation with disrupted hippocampal development in mice. *Nutrition* **32**, 1019–1027 (2016).

91. Taketo, M. *et al.* FVB/N: An inbred mouse strain preferable for transgenic analyses. *Proc. Natl. Acad. Sci. U. S. A.* (1991) doi:10.1073/pnas.88.6.2065.

92. Pugh, P. L., Ahmed, S. F., Smith, M. I., Upton, N. & Hunter, A. J. A behavioural characterisation of the FVB/N mouse strain. *Behav. Brain Res.* **155**, 283–289 (2004).

93. Wong, K. *et al.* Sequencing and characterization of the FVB/NJ mouse genome. *Genome Biol.* **13**, (2012).

94. Petrosino, J. M. *et al.* Graded Maximal Exercise Testing to Assess Mouse Cardio-Metabolic Phenotypes. *PLoS One* **11**, e0148010 (2016).

95. Wang, M. *et al.* Sharing and community curation of mass spectrometry data with Global Natural Products Social Molecular Networking. *Nat. Biotechnol.* **34**, 828–837 (2016).

96. T'Kindt, R. & Van Bocxlaer, J. LC-MS based metabolomics. in *Handbook on Mass Spectrometry: Instrumentation, Data and Analysis, and Applications* (2010). doi:10.1039/c1mb05350g.

97. Daviss, B. Growing pains for metabolomics. *Scientist* (2005).

98. Pluskal, T., Castillo, S., Villar-Briones, A. & Orešič, M. MZmine 2: Modular framework for processing, visualizing, and analyzing mass spectrometry-based molecular profile data. *BMC Bioinformatics* (2010) doi:10.1186/1471-2105-11-395.

99. Langley-Evans, S. C. Developmental programming of health and disease. *Proc. Nutr. Soc.* **65**, 97–105 (2006).

100. Mayneris-Perxachs, J. & Swann, J. R. Metabolic phenotyping of malnutrition during the first 1000 days of life. *European Journal of Nutrition* vol. 58 909–930 (2019).

101. Fernandez-Twinn, D. S. *et al.* The maternal endocrine environment in the low-protein model of intra-uterine growth restriction. *Br. J. Nutr.* (2003) doi:10.1079/bjn2003967.

102. Yamashiro, Y., Nagpal, R. & Nagata, S. Metabolic disease: Obesity, malnutrition, and intestinal microbiota. *Journal of Pediatric Biochemistry* (2015) doi:10.1055/s-0035-1564577.

103. Vítek, L. & Haluzík, M. The role of bile acids in metabolic regulation. *Journal of Endocrinology* vol. 228 R85–R96 (2016).

104. Urdaneta, V. & Casadesús, J. Interactions between bacteria and bile salts in the gastrointestinal and hepatobiliary tracts. *Frontiers in Medicine* vol. 4 (2017).

105. Li, H. *et al.* Characteristics of the intestinal microbiota in very low birth weight infants with extrauterine growth restriction. *Front. Pediatr.* (2019) doi:10.3389/fped.2019.00099.

106. WHO. *WHO | UNICEF-WHO-The World Bank: Joint child malnutrition estimates - Levels and trends*. *WHO* (World Health Organization, 2019).

107. Barker, D. J. P. & Osmond, C. INFANT MORTALITY, CHILDHOOD NUTRITION, AND ISCHAEMIC HEART DISEASE IN ENGLAND AND WALES. *Lancet* (1986)

doi:10.1016/S0140-6736(86)91340-1.

108. Godfrey, K. M. & Barker, D. J. Fetal nutrition and adult disease. *Am. J. Clin. Nutr.* **71**, 1344S-1352S (2000).

109. United Nations Children's Fund (UNICEF) World Health Organization & International Bank for Reconstruction and Development/The World Bank. Levels and trends in child malnutrition: key findings of the 2018 Edition of the Joint Child Malnutrition Estimates. 1–16 (2018) doi:10.1016/S0266-6138(96)90067-4.

110. Song, L., Johnson, M. D. & Tamashiro, K. L. K. *Maternal and Epigenetic Factors That Influence Food Intake and Energy Balance in Offspring*. *Appetite and Food Intake: Central Control* (2017).

111. Wells, J. C. K. The thrifty phenotype: An adaptation in growth or metabolism? *Am. J. Hum. Biol.* **23**, 65–75 (2011).

112. Hales, C. N. & Barker, D. J. P. The thrifty phenotype hypothesis. *Br. Med. Bull.* (2001) doi:10.1093/bmb/60.1.5.

113. Kovatcheva-Datchary, P., Tremaroli, V. & Bäckhed, F. The gut microbiota. in *The Prokaryotes: Human Microbiology* (2013). doi:10.1007/978-3-642-30144-5_87.

114. Chassaing, B. & Gewirtz, A. T. Gut Microbiome and Metabolism. in *Physiology of the Gastrointestinal Tract: Sixth Edition* vols 1–2 775–793 (Elsevier Inc., 2018).

115. Hsu, B. *et al.* Bacteriophages dynamically modulate the gut microbiota and metabolome. *bioRxiv* (2018) doi:10.1101/454579.

116. Quinn, R. A. *et al.* Global chemical effects of the microbiome include new bile-acid conjugations. *Nature* **579**, (2020).

117. Pathak, P. *et al.* Intestine farnesoid X receptor agonist and the gut microbiota activate G-protein bile acid receptor-1 signaling to improve metabolism. *Hepatology* (2018) doi:10.1002/hep.29857.

118. Durack, J. & Lynch, S. V. The gut microbiome: Relationships with disease and opportunities for therapy. *Journal of Experimental Medicine* vol. 216 20–40 (2019).

119. Kang, D. W. *et al.* Microbiota Transfer Therapy alters gut ecosystem and improves gastrointestinal and autism symptoms: An open-label study. *Microbiome* (2017) doi:10.1186/s40168-016-0225-7.

120. Bajaj, J. S. *et al.* Fecal microbiota transplant from a rational stool donor improves hepatic encephalopathy: A randomized clinical trial. *Hepatology* (2017) doi:10.1002/hep.29306.

121. Pekmez, C. T., Dragsted, L. O. & Brahe, L. K. Gut microbiota alterations and dietary modulation

in childhood malnutrition – The role of short chain fatty acids. *Clin. Nutr.* (2018) doi:10.1016/J.CLNU.2018.02.014.

122. Lin, S. *et al.* Undernutrition Shapes the Gut Microbiota and Bile Acid Profile in Association with Altered Gut-Liver FXR Signaling in Weaning Pigs. *J. Agric. Food Chem.* (2019) doi:10.1021/acs.jafc.9b01332.

123. Yang, J., Qian, K., Wang, C. & Wu, Y. Roles of Probiotic Lactobacilli Inclusion in Helping Piglets Establish Healthy Intestinal Inter-environment for Pathogen Defense. *Probiotics and Antimicrobial Proteins* (2018) doi:10.1007/s12602-017-9273-y.

124. Weaver, C. M. Diet, Gut Microbiome, and Bone Health Gut Mirobiome-a New Frontier? HHS Public Access. *Curr Osteoporos Rep* (2015) doi:10.1007/s11914-015-0257-0.

125. Friedman, J. E. Developmental programming of obesity and diabetes in mouse, monkey, and man in 2018: Where are we headed? *Diabetes* (2018) doi:10.2337/dbi17-0011.

126. E., P., T., V. M., S.J., L. & K.L., C. Does maternal malnutrition impact pathways involved in folate production and transport? *Reprod. Sci.* (2018).

127. Gohir, W. *et al.* Pregnancy-related changes in the maternal gut microbiota are dependent upon the mother's periconceptional diet. *Gut Microbes* **6**, 310–320 (2015).

128. Milani, C. *et al.* The First Microbial Colonizers of the Human Gut: Composition, Activities, and Health Implications of the Infant Gut Microbiota. (2017) doi:10.1128/MMBR.

129. Li, H. *et al.* Characteristics of the intestinal microbiota in very low birth weight infants with extrauterine growth restriction. *Front. Pediatr.* **7**, (2019).

130. Braun, K. V. *et al.* Dietary Intakes of Folic Acid and Methionine in Early Childhood Are Associated with Body Composition at School Age. *J. Nutr.* **145**, 2123–2129 (2015).

131. Allen, L. H. B Vitamins in Breast Milk: Relative Importance of Maternal Status and Intake, and Effects on Infant Status and function. *Adv. Nutr.* (2012) doi:10.3945/an.111.001172.

132. Swaminathan, S., Thomas, T. & Kurpad, A. V. B-vitamin interventions for women and children in low-income populations. *Current Opinion in Clinical Nutrition and Metabolic Care* (2015) doi:10.1097/MCO.0000000000000166.

133. Henderson, A. M., Aleliunas, R. E., Tai, D. C., Chem, N. G. J. & Green, T. J. The role of insulin-like growth factor-1 in programming of offspring adiposity by maternal folate/ vitamin B12 imbalance. *FASEB J.* (2016).

134. Lang, D. H. *et al.* Adjusting data to body size: a comparison of methods as applied to quantitative

trait loci analysis of musculoskeletal phenotypes. *J. Bone Miner. Res.* **20**, 748–57 (2005).

135. Thompson, L. R. *et al.* A communal catalogue reveals Earth's multiscale microbial diversity. *Nature* (2017) doi:10.1038/nature24621.

136. Gonzalez, A. *et al.* Qiita: rapid, web-enabled microbiome meta-analysis. *Nat. Methods* **15**, 796–798 (2018).

137. Xiao, J. F., Zhou, B. & Ressom, H. W. Metabolite identification and quantitation in LC-MS/MS-based metabolomics. *TrAC - Trends in Analytical Chemistry* (2012) doi:10.1016/j.trac.2011.08.009.

138. Kirshner, Z. Z. & Gibbs, R. B. Use of the REVERT ® total protein stain as a loading control demonstrates significant benefits over the use of housekeeping proteins when analyzing brain homogenates by Western blot: An analysis of samples representing different gonadal hormone states. *Mol. Cell. Endocrinol.* **473**, 156–165 (2018).

139. Smith, H. W. An ErbB2/c-Src axis links bioenergetics with PRC2 translation to drive epigenetic reprogramming and mammary tumorigenesis. doi:10.1038/s41467-019-10681-4.

140. Tzimas, C. *et al.* WIPI1 is a conserved mediator of right ventricular failure. *JCI Insight* **4**, (2019).

141. Bowles, J. *et al.* Retinoic Acid Antagonizes Testis Development in Mice. *CellReports* **24**, 1330–1341 (2018).

142. Knight, R. *et al.* Best practices for analysing microbiomes. *Nature Reviews Microbiology* vol. 16 (2018).

143. Chong, J. *et al.* MetaboAnalyst 4.0: Towards more transparent and integrative metabolomics analysis. *Nucleic Acids Res.* (2018) doi:10.1093/nar/gky310.

144. Yatsunenko, T. *et al.* Human gut microbiome viewed across age and geography. *Nature* **486**, 222–7 (2012).

145. Dominguez-Bello, M. G., Godoy-Vitorino, F., Knight, R. & Blaser, M. J. Role of the microbiome in human development. *Gut* (2019) doi:10.1136/gutjnl-2018-317503.

146. Gilbert, J. A. *et al.* Microbiome-wide association studies link dynamic microbial consortia to disease. *Nature* **535**, 94–103 (2016).

147. Smith-Brown, P., Morrison, M., Krause, L. & Davies, P. S. W. Mothers secretor status affects development of childrens microbiota composition and function: A pilot study. *PLoS One* **11**, (2016).

148. Wang, X. & Gibson, G. R. Effects of the in vitro fermentation of oligofructose and inulin by bacteria growing in the human large intestine. *J. Appl. Bacteriol.* (1993) doi:10.1111/j.1365-2672.1993.tb02790.x.

149. Adamberg, S. *et al.* Degradation of Fructans and Production of Propionic Acid by Bacteroides thetaiotaomicron are Enhanced by the Shortage of Amino Acids. *Front. Nutr.* **1**, (2014).

150. Rios-Covian, D. *et al.* Different metabolic features 1 of Bacteroides fragilis growing in the presence of glucose and exopolysaccharides of bifidobacteria. *Front. Microbiol.* **6**, (2015).

151. Fan, W., Tang, Y., Qu, Y., Cao, F. & Huo, G. Infant formula supplemented with low protein and high carbohydrate alters the intestinal microbiota in neonatal SD rats. *BMC Microbiol.* (2014) doi:10.1186/s12866-014-0279-2.

152. Ventura, M. *et al.* Gut Bifidobacteria Populations in Human Health and Aging. (2016) doi:10.3389/fmicb.2016.01204.

153. Rios-Covian, D., Salazar, N., Gueimonde, M. & de los Reyes-Gavilan, C. G. Shaping the Metabolism of Intestinal Bacteroides Population through Diet to Improve Human Health. *Front. Microbiol.* **8**, 376 (2017).

154. Belenguer, A. *et al.* Impact of pH on Lactate Formation and Utilization by Human Fecal Microbial Communities. *Appl. Environ. Microbiol.* **73**, 6526–6533 (2007).

155. Macy, J. M., Ljungdahl, L. G. & Gottschalk, G. Pathway of succinate and propionate formation in Bacteroides fragilis. *J. Bacteriol.* (1978) doi:10.1128/jb.134.1.84-91.1978.

156. Ciarlo, E. *et al.* Impact of the microbial derived short chain fatty acid propionate on host susceptibility to bacterial and fungal infections in vivo. *Sci. Rep.* **6**, 37944 (2016).

157. Mejía-León, M. E. & Calderón de la Barca, A. M. Diet, microbiota and immune system in type 1 diabetes development and evolution. *Nutrients* vol. 7 9171–9184 (2015).

158. Wang, C. Y., Liu, S., Xie, X. N. & Tan, Z. R. Regulation profile of the intestinal peptide transporter 1 (PepT1). *Drug Design, Development and Therapy* (2017) doi:10.2147/DDDT.S151725.

159. Fox, I. S. Riboflavin deficiency. *British Medical Journal* vol. 2 678 (1942).

160. Van Gammeren, D. Vitamins and minerals. in *Essentials of Sports Nutrition and Supplements* (2008). doi:10.1007/978-1-59745-302-8_15.

161. Martínez, Y. *et al.* The role of methionine on metabolism, oxidative stress, and diseases. *Amino Acids* (2017) doi:10.1007/s00726-017-2494-2.

162. Zou, K., Ouyang, Q., Li, H. & Zheng, J. A global characterization of the translational and transcriptional programs induced by methionine restriction through ribosome profiling and RNA-seq. *BMC Genomics* (2017) doi:10.1186/s12864-017-3483-2.

163. Semba, R. D. *et al.* Child Stunting is Associated with Low Circulating Essential Amino Acids. *EBioMedicine* **6**, (2016).

164. Kalhan, S. C. & Marczewski, S. E. Methionine, homocysteine, one carbon metabolism and fetal growth. *Reviews in Endocrine and Metabolic Disorders* (2012) doi:10.1007/s11154-012-9215-7.

165. Magnúsdóttir, S., Ravcheev, D., De Crécy-Lagard, V. & Thiele, I. Systematic genome assessment of B-vitamin biosynthesis suggests cooperation among gut microbes. *Front. Genet.* **6**, (2015).

166. Chan, J. *et al.* Low dietary choline and low dietary riboflavin during pregnancy influence reproductive outcomes and heart development in mice. *Am. J. Clin. Nutr.* (2010) doi:10.3945/ajcn.2009.28754.

167. Ye, J. *et al.* Butyrate Protects Mice Against Methionine–Choline-Deficient Diet-Induced Non-alcoholic Steatohepatitis by Improving Gut Barrier Function, Attenuating Inflammation and Reducing Endotoxin Levels. *Front. Microbiol.* **9**, (2018).

168. Gregersen, N. Riboflavin-responsive defects of β-oxidation. *J. Inherit. Metab. Dis.* **8**, 65–69 (1985).

169. Kasahara, A. & Scorrano, L. Mitochondria: From cell death executioners to regulators of cell differentiation. *Trends in Cell Biology* (2014) doi:10.1016/j.tcb.2014.08.005.

170. Guitart-Mampel, M. *et al.* Mitochondrial implications in human pregnancies with intrauterine growth restriction and associated cardiac remodelling. *J. Cell. Mol. Med.* (2019) doi:10.1111/jcmm.14282.

171. Mandò, C. *et al.* Placental mitochondrial content and function in intrauterine growth restriction and preeclampsia. *Am. J. Physiol. - Endocrinol. Metab.* (2014) doi:10.1152/ajpendo.00426.2013.

172. Gomez, A. *et al.* Cysteine dietary supplementation reverses the decrease in mitochondrial ROS production at complex I induced by methionine restriction. *J. Bioenerg. Biomembr.* (2015) doi:10.1007/s10863-015-9608-x.

173. La Frano, M. R. *et al.* Diet-induced obesity and weight loss alter bile acid concentrations and bile acid–sensitive gene expression in insulin target tissues of C57BL/6J mice. *Nutr. Res.* (2017) doi:10.1016/j.nutres.2017.07.006.

174. Trauner, M., Claudel, T., Fickert, P., Moustafa, T. & Wagner, M. Bile Acids as Regulators of Hepatic Lipid and Glucose Metabolism. *Dig. Dis.* **28**, 220–224 (2010).

175. Zhou, X. *et al.* Evidence for liver energy metabolism programming in offspring subjected to intrauterine undernutrition during midgestation. *Nutr. Metab. (Lond).* **16**, 20 (2019).

176. Hasek, B. E. *et al.* Remodeling the integration of lipid metabolism between liver and adipose tissue by dietary methionine restriction in rats. *Diabetes* (2013) doi:10.2337/db13-0501.

177. Di Ciaula, A. *et al.* Bile acid physiology. *Ann. Hepatol.* **16**, (2017).

178. Chiang, J. Y. L. Bile acid metabolism and signaling. *Compr. Physiol.* **3**, 1191–212 (2013).

179. Fuchs, C., Claudel, T. & Trauner, M. Bile acid-mediated control of liver triglycerides. *Semin. Liver Dis.* (2013) doi:10.1055/s-0033-1358520.

180. Morales, A. J., Haubricht, R. H., Hwang, J. Y., Asakura, H. & Yen, S. S. C. The effect of six months treatment with a 100 mg daily dose of dehydroepiandrosterone (DHEA) on circulating sex steroids, body composition and muscle strength in age-advanced men and women. *Clin. Endocrinol. (Oxf).* (1998) doi:10.1046/j.1365-2265.1998.00507.x.

181. Morales, A. J., Nolan, J. J., Nelson, J. C. & Yen, S. S. C. Effects of replacement dose of dehydroepiandrosterone in men and women of advancing age. *J. Clin. Endocrinol. Metab.* (1994) doi:10.1210/jcem.78.6.7515387.

182. Weiss, E. P., Villareal, D. T., Fontana, L., Han Dong-Ho, D. H. & Holloszy, J. O. Dehydroepiandrosterone (DHEA) replacement decreases insulin resistance and lowers inflammatory cytokines in aging humans. *Aging (Albany. NY).* (2011) doi:10.18632/aging.100327.

183. Barrett-Connor, E., Khaw, K. T. & Yen, S. S. c. A Prospective Study of Dehydroepiandrosterone Sulfate, Mortality, and Cardiovascular Disease. *N. Engl. J. Med.* (1986) doi:10.1056/NEJM198612113152405.

184. Labrie, F. *et al.* Endocrine and intracrine sources of androgens in women: Inhibition of breast cancer and other roles of androgens and their precursor dehydroepiandrosterone. *Endocrine Reviews* (2003) doi:10.1210/er.2001-0031.

185. Yang, Y. L. *et al.* Deficiency of Gpr1 improves steroid hormone abnormality in hyperandrogenized mice. *Reprod. Biol. Endocrinol.* (2018) doi:10.1186/s12958-018-0363-9.